university of groningen / faculty of science and engineering

Research Thesis

Final report

The effectiveness of travel restricting measures against COVID-19

A Metapopulation model

Author:
Tom Venema s3872718

Supervisors:
Dr. N. (Nima) Monshizadeh Naini
Prof. dr. M. (Ming) cao

Groningen, March 2021

MSc Industrial Engineering and Management
Faculty of Science and Engineering
University of Groningen

Abstract

Keywords— COVID-19, SIDARE model, flux control

The recent COVID-19 pandemic leads to global social and economic disruption. Decision-makers continuously face the challenge of choosing the right mitigating strategies to fight the pandemic. One strategy that is still not fully understood is the effectiveness of implementing travel restrictions at the early stage of the spreading. Therefore, this report simulates different travel restricting measures and evaluates their effectiveness. The simulation is done by creating a novel metapopulation SIDARE model. This model captures the effect of travel on the spreading of COVID-19 in the Netherlands and is able to describe the evolution of the pandemic accurately. It is found that travel restricting measures on themselves delays, but not mitigates, infections. Moreover, the most effective way to implement travel restrictions is regional, in the province where the initial infection occurred. When 99 % of the travel from and to that region is reduced, a delay of 48 days on the national infection peak can be achieved. Finally, the usefulness of this delay is studied by combining travel restricting measures with different vaccination strategies. It is found that travel restricting measures can be used to increases the potential lives saved by vaccinating.

Acknowledgements

In front of you lies the report 'The effectiveness of travel restricting measures against COVID-19'. This report is written in the context of completing my research project. The research project is a requirement for obtaining my master degree 'Industrial Engineering and Management' at the Rijksuniversiteit Groningen.

The current corona pandemic caused some extra challenges during this research project. The lack of physical contact with friends, family and other students impacted my overall motivation. Nevertheless, I'm am really proud of the result, and I am looking back at an enjoyable and learning-full experience.

I would like to thank my supervisors Dr. N.(Nima) Monshizadeh Naini and Prof. dr. M.(Ming) cao for allowing me to conduct this research. Especially, I would like to thank my 1st supervisor Dr. N.(Nima) Monshizadeh Naini, for his excellent guidance and his genuine interest in his students. Gijs Disselhorst deserves a special note because he always took the time to discuss my ideas. At last, I would like to thank my friends and family who supported me during this process.

I hope you enjoy your reading.

Tom Venema March 24, 2021

Contents

List of Figures

List of Tables

Chapter 1: Introduction

In December 2019, a novel coronavirus called SARS-COV-2 arose in Wuhan, China. The virus is highly contagious and causes the disease COVID-19 through human-to-human transmission. On 12 March, The World Health Organization (WHO) officially characterized COVID-19 as a pandemic (WHO, 2020a) and by 18 October 2020, more than 40 million cases were confirmed with nearly 1.1 million deaths. (WHO, 2020b). In order to reduce the spreading of COVID-19, countries implement non-pharmaceutical intervention policies (NPIs). Some examples of NPIs are social distancing, the closing of public places, and lock-downs. The decision on the duration and intensity of the NPIs differ per country. Spreading disease models take an essential role in this decision process (Nowzari et al., 2016). Spreading disease models capture the dynamics of disease and use them to study how diseases evolve. This information can be used by public health authorities to predict necessities during an outbreak. Subsequently, by combining real-world data, these models can evaluate the effectiveness of taken NPIs.

The most well-known spreading disease model is the simple SIR model, which describes how diseases evolve using three differential equations (Kermack and McKendrick, 1927). This model can roughly estimate the evolution of a disease. Since then, many studies have been conducted on improving this model. For example, the SEIR model by Hethcote and Van den Driessche (1991) is such an improvement. This model captures the disease's properties that there is a delay between being infected and being infectious, resulting in more accurate predictions. Later, more advanced models were created. These models are now often used to study the effects of disease-fighting strategies. Giordano et al. (2020) made the extended SIDARTHE model, which studies the effectiveness of contract tracing policies. Furthermore, Djidjou Demasse et al. (2020) made the SEAIRD model, which studies the optimal control strategy until vaccine deployment.

Fewer models take spatial dynamics into consideration. An important contribution in this field has been done by Gatto et al. (2020), who uses the SEPIAHQRD model to simulate the effectiveness of localized containment measures. Della Rossa et al. (2020) uses a spatial model to develop a differentiated feedback control strategy for fighting the COVID-19 pandemic using regional containment measures. Using this strategy, they found that the total number of infected and deceased cases will be almost the same as when a national lock-down strategy is taken. However, the differentiated strategy significantly reduces economic costs. Very little work has been done on the effectiveness of travel restricting measures. Chinazzi et al. (2020) did study the effectiveness of travel restricting measure taken by the government. They found that the taken measures only delayed the spreading of the disease by 3 to 5 days. However, this travel ban was executed after the disease already spread throughout the whole country. A natural question that rises would be: would the travel restricting measures be effective if they were taken on time, or are they not effective at all?

In this report, the existing SIDARE model will be upgraded to a metapopulation SIDARE model. The metapopulation SIDARE model can model the effects of travel between regions on the spreading of the disease. This model is then used to simulate travel restricting measures for four different cases. These different cases give insights into which way travel restricting measures should be implemented by the government. The novelty of this report is that it studies travel restricting measures if they were taken on time. Moreover, this report is the first to study if these effects can be used to save lives (to the best of my knowledge).

In the rest of this chapter, the problem and goal statements are formulated, which lead to the research questions. Then, a brief methodology will be given on these research questions will be answered. In chapter 2, a literature study is carried out. This literature study reviews the

existing models that are created throughout history. Chapter 3 describes the construction of the extended SIDARE model and validates the design. The model is then used to study different NPIs, which is described in chapter 4. In chapter 5, the combination of travel restricting measures and vaccination is studied. Finally, the conclusion, discussion, and future work are stated in chapter 6/7/8, respectively.

1.1 Problem context

"If we don't have a vaccine—yes, we are all going to get it" is an infamous quote by a doctor during the early stages of the SARS outbreak in 2002. This opinion was widely shared by many experts at that time, leading to great concern in public (Shaw, 2007). History has shown that this prediction was wrong. The misconception of the strength of the virus was partially due to modelling flaws. The models calculated an R_0 of 6, meaning that every individual would infect six others on average. Luckily, this number later happened to be far lower than that. Despite the calculation mistake, infectious disease models were also part of the solution. The models were used to predict which measures would be the most effective to fight the spreading—eventually leading to full containment of SARS.

This case stresses the impact of spreading disease models. Nowadays, during the COVID-19 pandemic, spreading disease models also play a significant role. Decision-makers continuously face the challenge of fighting the disease without harming the economy too much. They need to answer questions like: when and how long should schools, theatres, stores, and other public places be closed/opened? To what extend is it needed to force behavioural changes like wearing mouth masks or disinfecting hands? Should the necessary measures count for the whole nation or only for regions with many infections? All these decisions have a significant impact on the daily life of people and the economy. Therefore, the efficiency and efficacy of these measures have to be understood.

1.2 Scope

There are numerous factors that influence the spreading of a disease, which makes them hard to model. Pica and Bouvier (2012) describes different factors that influences the spreading. In this research, some of these factors are left out. The factors that are included and excluded are shown infigure 1.1. The focus of this report will be on the travel factor. By "travel" is meant: the movement of people within the Netherlands on a daily bases. Travel for a longer period (such as a vacation) or a short one time trip is excluded in this research. For simplicity, seasonality effects such as the weather are left out. Moreover, ventilation and other localized measures are not modelled.

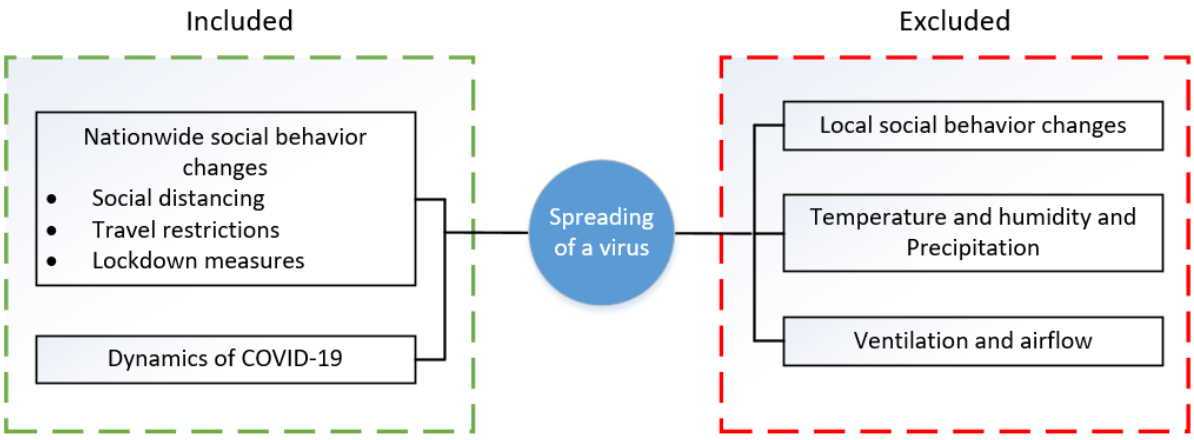

Figure 1.1: Scope of the research, showing which factors that influences the spreading of a disease are modeled in this research.

1.3 Goal statement

Based on the research background, the following goal statement is formulated

---

"Design a metapopulation SIDARE model which can be used to test and evaluate the effectiveness of travel restricting measures"

The focus of this report is to test whether travel restricting measures would be useful for fighting COVID-19 in the Netherlands. However, the designed model can also be used to study outbreaks of different disease in other countries.

1.4 Research approach

Choosing a research approach can help in keeping track of the bigger picture during a research (Van Aken and Berends, 2018). To determine which research approach will be taken, we will consider several aspects. The aspects are 1) Is this research practical or theory-oriented? 2) Is the origin of the problem known or not? 3) Can the problem be considered as an implementation problem?

1) This problem can be considered both practical and theory-oriented. Practical (known)solutions will be tested to test their effectiveness. However, studying the effects of travel on the spreading of diseases will result in insights that can be added to the knowledge base.

2) The origin of the problem seems logical. It is known that more travel leads to more infections. This means that there is no need for further investigating the origin of the problem. And thus, no diagnostic phase is needed.

3) This problem cannot be considered as an implementation problem. The implementing of travel restriction will be evaluated, but the actual implementation will obviously not been done in this research.

Considering these aspects, a logical research approach would be the design cycle (Wieringa, 2014). The design cycle is a part of the larger engineering cycle. However, the design cycle excludes the actual implementation and the implementation evaluation figure 1.2. The actual implementation will not be part of this project, so the design cycle is more suitable. Consequently, the design cycle is chosen over the problem-solving cycle of van Aken (Van Aken and Berends, 2018). The

problem-solving cycle includes a diagnostic phase. In this project, the origin of the problem is already known, so there is no need for a diagnostic phase. The design cycle of Wieringa implies that the project should contain the following phases: Problem investigation, treatment design, design evaluation. These phases are shortly summarized below

- **Problem investigation** To investigate the problem, a broad literature review will be carried out. This literature review will help in finding knowledge gaps and potential research opportunities
- **Treatment design** In this phase, the design requirements are defined. These design requirements will be used to make a new artefact.
- **Design evaluation** The created artefacts will be evaluated. This can be done by simulating the artefact. In this simulation, multiple KPI's can be compared to the earlier made requirements.

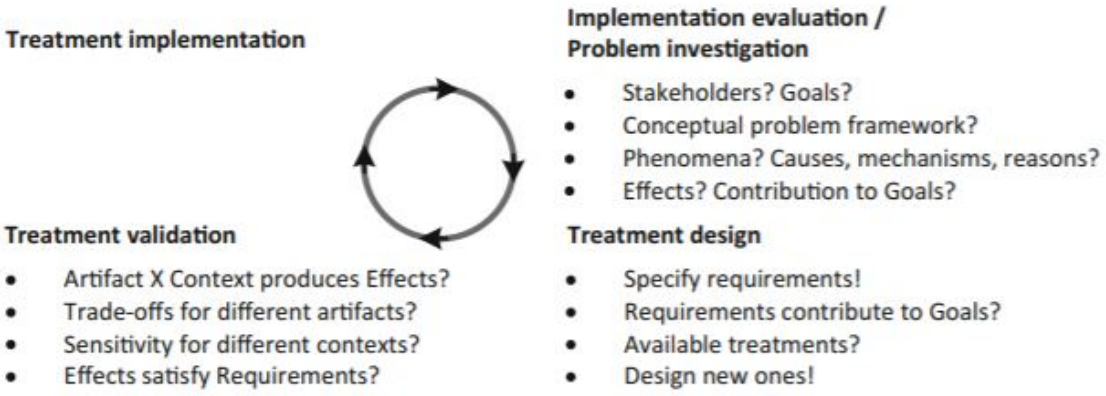

Figure 1.2: This picture shows the engineering cycle. Only the first three steps are taken, so the implementation and implementation validation steps are excluded. This smaller circle is called the design cycle (Wieringa, 2014)

Subsequently, these three main phases of the project lead to research questions. The research question are further elaborated in section 1.5.

1.5 Research questions and operationalization

In this section, the main research question is divided into five sub-questions. These sub-questions are then be further elaborated in each section. Finally, the tools that will be used for the operationalization are discussed. The main research question of this research is:

What is the effect of travel restricting measures in the Netherlands on the spreading of the COVID-19 pandemic?

To answer this question, five sub-questions will be answered
SQ1: *What spreading disease models exist, and what are their differences?*
SQ2: *How can a spreading disease model be constructed to study the effects of travel within the Netherlands?*
SQ3: *What different travel restricting measures can be thought of, and how effective will they be?*
SQ4: *Can the effects of travel restricting measures be used in fighting the pandemic?*

1.5.1 Sub-question 1: What spreading disease models exist, and what are their differences?

The goal here is to get insights on how to model the spreading of the COVID-19 pandemic. These insights will be obtained by exploring existing spreading disease models in the literature. The models will be compared in terms of how they work, their usefulness and their pros and cons.

1.5.2 Sub-question 2: How can a spreading disease model be constructed to study the effects of travel within the Netherlands

Out of the insights obtained is SQ1 requirements can be set up for a new model. This model will be created in Matlab. The existing SIDARE model will be recreated and extended to a version that contains travel between provinces. This model will be validated by remaking graphs of previously done research. After that, data will be obtained to simulate the spreading of COVID-19 in the Netherlands. The most important data that will be obtained is the movement of people between regions. This movement will be estimated by public commuting data.

1.5.3 Sub-question 3: What different travel restricting measures can be thought of, and how effective will they be?

To answer this sub-question, four different cases are simulated and evaluated.

- **Case I:** A Nationwide travel restriction will be enforced. Only people with vital professions (doctors, fireman etc.) will be allowed to travel. The travel restriction will vary from light travel restriction (0% of the reference travel) up to a complete travel ban (99% of the reference travel).
- **Case II:** Travel restriction will be enforced by isolating one province from the rest of the Netherlands. The travel restriction will vary from light travel restriction (0% of the reference travel) up to a complete travel ban (99% of the reference travel). This simulation will be done for every province.
- **Case III:** In this case the Netherlands will be split into two clusters: the Northeast and the Southwest. People are only allowed to travel within their cluster, but not to the other. It can be argued that less travel is needed when the clusters are this big. Therefore, it is decided only to simulate a complete travel ban of 99% of the reference travel.
- **Case IV:** In this case, the Netherlands will also be split into two clusters. However, in this case, 'smarter' clusters are chosen. Here, the clusters consist of the provinces that have

the most travel between them. In this case, it is also decided to enforce a complete travel ban of 99% of the reference travel.

For every scenario, the total amount of infected and deceased people will be calculated. Every measure's effectiveness will be evaluated by analyzing the total amount of infected, deceased, or the infection peak's timing. This will be compared to the control effort needed for that measure. After that, the robustness of each measure will be tested through a parameter variation study. The infectiousness of COVID-19 can change naturally (mutation or weather) or through taken NPIs by the government. Therefore, the parameter variation evaluates the travel restricting measure when these conditions change.

1.5.4 Sub-question 4: Can the effects of travel restricting measures be used in fighting the pandemic?

To answer this question, a fifth case is set up. This case studies whether the effects found in case I - IV can be used to fight the pandemic. Chinazzi et al. (2020) showed that travel restrictions cause a delay in the infection. The time won by this delay can be used to vaccinate people. Therefore the different cases are now simulated together with a vaccination rate. This case will be evaluated by comparing the different amount of deceased expected due to COVID-19.

Chapter 2: Analysis spreading disease models

To get a better understanding of spreading disease models, the most relevant research in this field is analyzed. For every research, the used spreading disease model is analyzed and their contribution is summarized. A distinction is made between population models, network models and metapopulation models. At the end of the chapter, an overview of the models is given and the findings are summarized

2.1 Population models

The most prominent spreading disease models are 'agent based' or 'population' models. These models divides the population into different compartments, which represent the state of an agent. The most commonly used compartments are Susceptible (S) and Infected (I). The movement of the agent from susceptible to infect is called 'infection rate' and the movement from Infected to Susceptible is called 'curing rate'. These movements can either be deterministic or stochastic. Deterministic means that movement happens at a specific rate while stochastic assume that the state transition happens with a certain probability (Nowzari et al., 2016). The latter is more accurate to model a spreading disease because, in the real world, it is not always guaranteed that someone gets infected. However, when the population is large enough, the deterministic model suffices too. Often, stochastic models are created and then a deterministic approximation is made. This deterministic approximation makes the model easier to analyze. To understand the differences between spreading disease models, two terms have to be explained.

- **Initial/basic reproduction number** is a term that describes the strength of a disease (often denoted by R_0. A reproduction number of 1.6 means that 100 people infect 160 others on average. When the reproduction number is bigger than 1, the disease's spreading grows, and when it's lower than 1, the disease typically dies out.
- **Threshold conditions** are used to describe the requirements for a disease to reach certain equilibria. The two most described equilibria are disease-free and epidemic. A disease-free equilibrium occurs when a disease dies out, and epidemic equilibrium occurs the disease spreads.
- **Mean-field theory** uses assumptions to simplifies stochastic systems, which makes them easier to analyse.

2.1.1 SIR model

The most commonly known spreading disease model is the classical SIR model. The SIR model is a simplified model which divides the population into three compartments: Susceptible (S), Infected (I), or Removed (R)(Kermack and McKendrick, 1927). The susceptible represent individuals that have not been infected yet and are susceptible to the disease. The infected represents individuals who are infected and able to spread the disease. The Removed represents the individuals that are not susceptible to the disease anymore (immune or dead). Figure 2.1 shows the compartment and its interrelations on the left side and the corresponding differential equations on the right side.

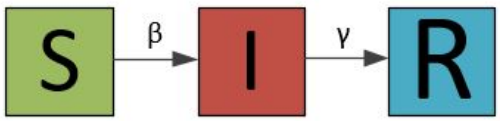

$$\begin{aligned} \dot{S} &= -\beta SI \\ \dot{I} &= \beta SI - \gamma I \\ \dot{R} &= \gamma I \end{aligned} \tag{2.1}$$

Figure 2.1: Schematic representation of the SIR model. Showing the compartments and its interrelations on the left and the corresponding differential equations on the right

The first equation describes the change of the S compartment over time $\dot{S}$. This depends on the amount of infected, amount of susceptible and the infection rate β. The infection rate β is a constant which is used to capture the infectiousness of a disease. The second equation describes the change of the I compartment over time $\dot{I}$. This depends on the amount of infected minus the amount of recovered. At last, the removed $\dot{R}$ over time is equal to the curing rate γ times the infected. It is important to notice that this is a very oversimplified infectious disease model. This model can roughly estimate the amount of susceptible, infected or recovered. However, it is important to know the limitations of this model. Some limitations are:

- This model assumes a constant homogeneous infectious and recovery rate, while in reality this varies.
- This model assumes that an infected individuals is immediately infectious. In reality there can be a certain delay.
- The model dependents on the 'best guess' of the parameters. These parameters can change and are often met with a certain uncertainty.

The basic reproduction number R_0 can be calculated $R_0 = \frac{\beta}{\gamma}$

2.1.2 SIS model

Influenza viruses are known to not confer long-lasting immunity, meaning that the SIR model does not suffice (Johnson et al., 2017). Therefore, the SIS (Susceptible-Infected-Susceptible) model is created. The first SIS model was described by Kermack and McKendrick (1927). Figure 2.2 shows the compartment and its interrelations on the left side and the corresponding differential equation on the right side.

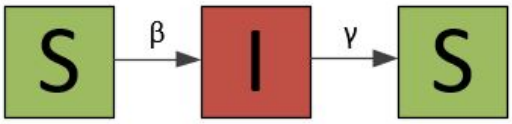

$$\begin{aligned} \dot{S} &= bI - aSI \\ \dot{I} &= aSI - bI \end{aligned} \tag{2.2}$$

Figure 2.2: Schematic representation of the SIS model. Showing the compartments and its interrelations on the left and the corresponding differential equations on the right

After analyzing these dynamics, it is found that when $\beta \leq \gamma$ the system will converge to a unique equilibrium of $x = 0$, where x represents the potion of the population infected. This implies that the disease dies out when. If $\beta > \gamma$, the system will converge to a unique equilibrium $x = (\beta - \gamma)/\beta$.

2.1.3 SEIR/SEIRS model

The SIR and the SIS model assume that an individual immediately becomes infectious when an individual gets infected. However, there is often a delay between those stages (called 'latent

period'). The SEIR/SEIRS model models the latent period by adding the 'E' compartment . The 'E' in the SEIR model stands for Exposed and represents the infected individuals who are not infectious. Figure 2.3 shows the compartments and its interrelations on the left side and the corresponding differential equations on the right side.

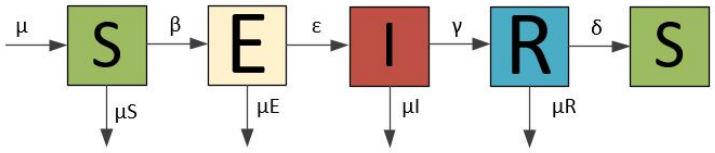

$$\begin{aligned}
&\dot{S}(t) + \dot{E}(t) + I(t) + \dot{R}(t) = 1 \\
&\dot{E} = \beta g(I)(1 - E - I - R) - (\epsilon + \mu)E \\
&\dot{I} = \epsilon E - (\gamma + \mu)I \\
&\dot{R} = \gamma I - (\delta + \mu)R
\end{aligned} \tag{2.3}$$

Figure 2.3: Schematic representation of the SEIRS model. Showing the compartments and its interrelations on the left and the corresponding differential equations on the right.

Hethcote and Van den Driessche (1991) studied the SIRS and SEIRS models properties when a nonlinear infection rate is applied. They argue that a bilinear infection rate, which is used by the SIR and SIS model, does not match real-world situations. They found that this nonlinear infection rate barley impacts the dynamical behaviour of the models. Moreover, they found that this model leads to multiple unique endemic equilibria. The equilibria are later proven to be globally stable by Li and Muldowney (1995). Later, Li et al. (1999) relaxes the assumption that the population size stays the same. In this model, the population size depends on time and whether the disease will become an endemic or not. They found endemic criteria dependent on the infected fraction of the population.

2.1.4 SEAIRD model

Djidjou Demasse et al. (2020) constructed the so-called SEAIRD model to study the optimal COVID-19 epidemic control until vaccine deployment. The compartments represent Susceptible (S) Exposed (E) Asymptomatic (A) Infected (I) Recovered (R) Dead (D). This model splits the infected cases into 'severe' and 'mild' cases, as shown in figure 2.9. The corresponding differential equations can be found in appendix A. The reason for this is that they argue that mild cases have significantly different characteristics than severe cases.

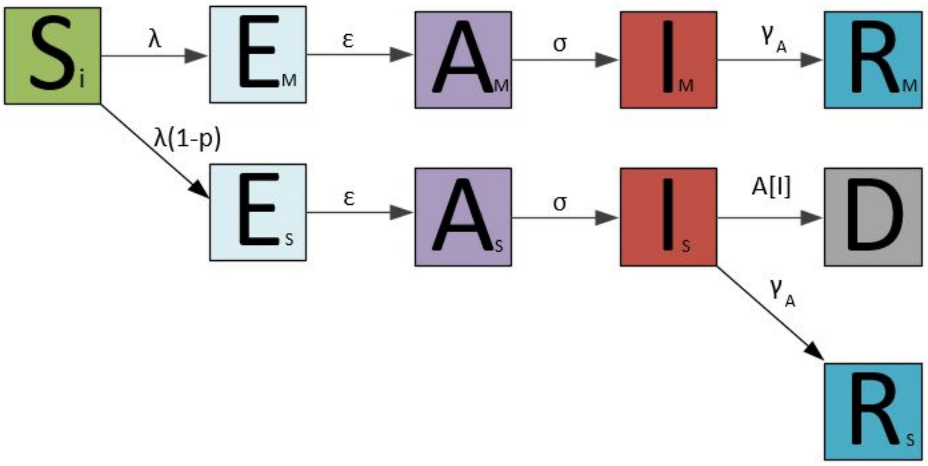

Figure 2.4: Schematic representation of the SEAIRD model. Showing the compartments and its interrelations.

In their research, they describe that there are two ways to halt the spread of an epidemic. The first one is by immunising the population through vaccines, and the second one is by achieving 'herd immunity'. The latter is studied in this paper. It is found that alleviate control too early only delays the epidemic wave. Also, varying the control over time provides the best results. The optimal control will be a short, intense control at the beginning of the period followed by a lower intermediate control.

2.1.5 SIDARTHE model

Giordano et al. (2020) made the so-called SIDARTHE model. This is a deterministic population model, dividing the population into eight compartments. The compartments of this model are: Susceptible (S), Infected(I) Diagnosed (D), Healed (H), Ailing (A), Recognized (R), Threatened (T), and Extinct (E). The compartments and their interrelations are shown in figure 2.5 and the corresponding differential equations in appendix A.

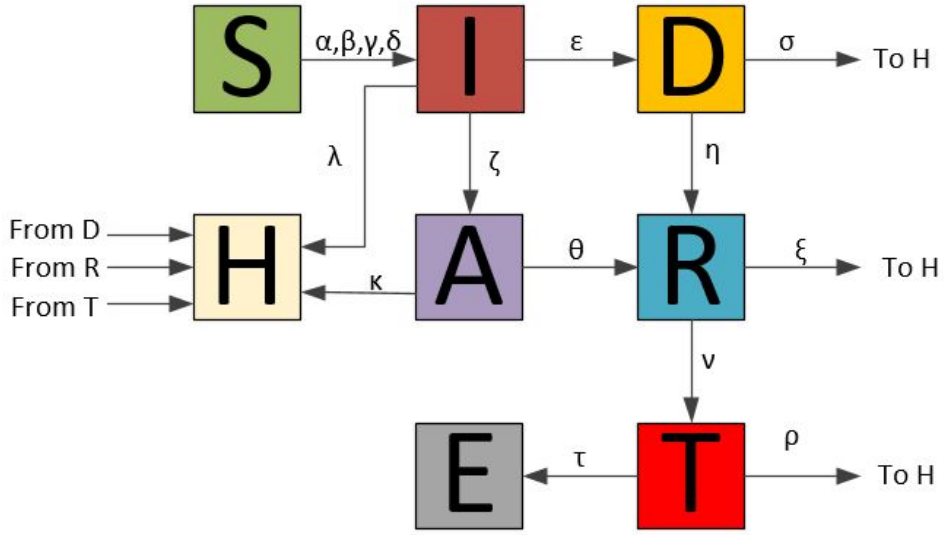

Figure 2.5: Schematic representation of the SIDHARTE model. Showing the compartments and its interrelations on the left and the corresponding differential equations on the right

The main contribution of this model is that it discriminates between detected and undetected infected. By doing so, diagnosing strategies can be studied. An example of this is studying the effects of contact tracing and testing. They found that when massive testing and contact tracing is applied, the lock-down can be weakened, and this will result in almost no extra deaths. This model can be extended to include co-existing disease, which can lead to a better approximation of the total collateral deaths. Co-existing diseases can lead to a faster-overloaded health care capacity, which results in indirectly COVID-19 deaths.

2.2 Network models

The drawbacks of the population models are that they assume a well-mixed population (homogeneity), which means that the movement from one compartment to another is equal for every individual. Not every individual has the same, for example, infection or curing rate in the real world. Therefore, network models are created. Network models consider the population by a connected graph $\mathcal{G} = (V, E)$ where V is the number of nodes (representing individuals) and E the number of edges (representing interactions). The adjacency matrix "A" describes

the interrelations between the nodes. The advantage of these models that state changing rates can differ per node. The infection rate in these models often dependents on the amount of neighbouring infected nodes—these aspect results in more heterogeneity, and better match the real world.

2.2.1 Network topologies

The topology of a network can significantly impact the strength of a virus propagation (Ganesh et al., 2005). The most common topologies are random homogeneous networks, small-world networks and heavy-tailed networks. To understand the differences between network topologies, several graph properties have to be defined.

- **The degree** of a node in an undirected graph is the sum of all neighbours of the node. In a directed graph, the degree is the number of edges pointing towards the node.
- **The average degree** of a graph is the sum of all the node's degree divided by the number of nodes.
- **The shortest path** Is the minimum amount of 'steps' between a pair of nodes.
- **The average path length** is the sum of the minimum amount of node steps between each pair of nodes divided by the total amount of shortest paths.
- **The clustering coefficient** is a measure to define how much a node tend to cluster. Node V's clustering coefficient is the fraction of the number of possible interconnections between node V and its neighbours. The clustering coefficient can be calculated by (2.4)

$$\frac{\text{(Number of links between the neighbors of V) * 2}}{\text{(Degree of node V)}*\text{(Degree of node V - 1)}} \tag{2.4}$$

Random homogeneous networks.
A Random homogeneous network is characterized that every node has the approximately same degree. The clustering coefficient is given by the network $\frac{\langle k \rangle}{N}$, where $\rangle k \langle$ denotes the average degree and N the total amount of nodes. The average shortest path is given by $\langle l \rangle = logN/log\langle l \rangle$, where $\langle l \rangle$ represents the average shortest path (Dorogovtsev, 2010). Real-world properties like high clustering coefficients are absent in this model

Small-world networks
The small-world network is a network where most of the nodes are not neighbours of each other, but a small number of steps can reach every node (Watts and Strogatz, 1998). This network is generated by an ordered lattice of hubs (a group of nodes with a high clustering coefficient). Between these hubs, several "short cuts" are generated, which significantly reduces the average path length. The result is a network with a high average clustering coefficient and a low average path length. Small-world characteristics are often found in website-links or social networks.

Heavy-tailed Networks
Heavy-tailed networks are networks where the degree of the nodes follow the power-law distribution. The power-law imposes that new nodes tend to connect with nodes that have already a higher degree. This preferential attachment causes a network to be highly centralized. Many real-world networks are considered "scale-free" (Pastor-Satorras et al., 2015). Scale-free networks follow the power-law distribution ($P(k) = k^{-\gamma}$) with power-law exponent γ taking a value between 2 and 3.

Time-varying networks
The topologies described above assume that the network is static. However, in the real world,

interactions between individuals change over time. If someone gets infected, it is logical that he/she temporary cuts connections with others. Therefore, some researchers study the effects of time varying topologies.

2.2.2 Network SIS model

Kephart and White (1992) constructed a network SIS model, which formed the basis of a large class of mean field models. This model is described by equation (2.5). Here, y denotes the fraction of infected nodes, k the average in-degree of each node, β the infection rate, and δ the curing rate.

$$\dot{y} = \beta k y(1-y) - \delta y \tag{2.5}$$

Kephart and White (1992) applied this model on a random homogeneous network and found an epidemic threshold of $\tau_c = \frac{1}{k}$. However, this thresholds only holds for random homogeneous networks.

Discrete-time network SIS model

Wang et al. (2003) created a discrete-time network SIS model to study the spreading of a virus in various networks. The infection and curing of each node happen with a probability described by equation (2.6) and equation (2.7) respectively. Here, $p_{i,t}$ denotes the probability that node i is infected at time t, and $\zeta_{i,t}$ the probability that node i does not receive infections from its neighbors at t.

$$\begin{aligned} \zeta_{i,t} &= \prod_{j:neighbor\ \text{of}\ i} \left(p_{j,t-1}(1-\beta) + (1-p_{j,t-1})\right) \\ &= \prod_{j:neighbor\ of} (1 - \beta * p_{j,t-1}) \end{aligned} \tag{2.6}$$

$$\begin{aligned} 1 - p_{i,t} = &(1-p_{i,t-1})\,\zeta_{i,t} + \delta p_{i,t-1}\zeta_{i,t} \\ &+ \frac{1}{2}\delta p_{i,t-1}\,(1-\zeta_{i,t}) \quad i = 1 \ldots N \end{aligned} \tag{2.7}$$

After conducting simulations on different topologies (random homogeneous and heavy-tailed), they found that the epidemic threshold can be described using only one parameter for both topologies. The epidemic threshold can be described by $\tau = 1/\lambda_{1,A}$, where $\lambda_{1,A}$ corresponds to the eigenvalue of the graph. Subsequently, they found that below this epidemic threshold, the number of infections decreases exponentially

Continues-time network SIS model

Van Mieghem et al. (2008) describes the continuous N-intertwined Markov-chain SIS model. In contradiction to previous papers, only one mean-field approximation is made in the derivations of this model. The mean-field assumption holds that a nodes infection rate is the average of the infected neighbours instead of a random variable. The resulting probability P_i that node i is infected can be described by equation (2.21).

$$\dot{p}_i = -\delta p_i + \sum_{j=1}^{N} a_{ij}\beta p_j\,(1-p_i) \tag{2.8}$$

Here is δ the recovery rate, β the infection rate, and a_{ij} the corresponding adjacency matrix. They found that if the virus strength is smaller than the epidemic threshold ($\tau < \tau_c$), the N-intertwined Markov chain is very accurate. If $\tau > \tau_c$, the N-intertwined Markov chain is only accurate if the network size is big enough. The stability properties for both the continues and discrete-time are later studied by Ahn and Hassibi (2013).

SIS dynamics on adaptive topology
Gross et al. (2006) studied the effect of adaptive topology on the SIS dynamics. In this model, a link between susceptible and infected can be removed, and the susceptible node can be rewired to another random susceptible node. The real-world application of this feature is that susceptible individuals can avoid infected individuals. After analyzing this model, new threshold conditions and properties are found. It is found that the epidemic threshold increases, limiting the chance of an epidemic.

2.2.3 Network SIR model

Moreno et al. (2002) Studied epidemic outbreaks on complex networks using the SIR model. The SIR model is applied to two complex networks: the Watts-Strogatz model and the Barab'asi-Albert. The Watts-Strogatz network is a small-world network with bounded connectivity, and the Barab' asi-Albert is a scale-free network. The network SIR model is described by

$$\frac{\mathrm{d}\rho_k(t)}{\mathrm{d}t} = -\rho_k(t) + \lambda k S_k(t)\Theta(t) \tag{2.9}$$

$$\frac{\mathrm{d}S_k(t)}{\mathrm{d}t} = -\lambda k S_k(t)\Theta(t) \tag{2.10}$$

$$\frac{\mathrm{d}R_k(t)}{\mathrm{d}t} = \rho_k(t) \tag{2.11}$$

In their research, they showed that the topology of a network greatly influences the behaviour of spreading. The Watts-Strogatz model's epidemic threshold is described by equation (2.12) and the epidemic threshold for the Barab 'asi-Albert by equation (2.13). However, if the model uses an infinitely large scale-free network, the disease will spread unconditionally. This means that there will not be an epidemic threshold.

$$\lambda_c = \frac{\langle k \rangle}{\langle k^2 \rangle} = \frac{2}{1 + 4m} \tag{2.12}$$

$$\lambda_c(N) \sim \frac{1}{\log N} \tag{2.13}$$

Effect of time delay
Xia et al. (2012) studied the effect of time delay on the epidemic properties within a network SIR model. They made an extended SIR model, which contains three infection states. This model is then be analyzed and simulated for two different topologies: homogeneous and heterogeneous. It is found that the effect of time delay significantly impact the epidemic threshold conditions. The new epidemic threshold are described by equation (2.14) for homogeneous topologies and by equation (2.15) for heterogeneous topologies.

$$\lambda > \lambda_c = \frac{\frac{1}{T+1} - \beta_1\beta_2}{\langle k \rangle} \qquad (2.14) \qquad \lambda > \lambda_c = \frac{\langle k \rangle}{\langle k^2 \rangle}\left(\frac{1}{T+1} - \beta_1\beta_2\right) \qquad (2.15)$$

Where in this case λ represents the effective strength (normally R_0), T represents the time delay, β represents the propagation vector and $\langle k \rangle$ represents the average degree. After simulating the dynamics some interesting conclusion have been found. Time delay between transmissions leads to a higher infection level and a lower epidemic threshold. Moreover, the introduction of a propagation vector accelerates the spreading of the disease.

2.2.4 Network G-SEIV model

Nowzari et al. (2014) constructed the generalized network SEIV model (G-SEIV). In contrast to the SEIR/SEIRS model, this model captures the possibility that someone can be infected but not be aware of it. This unawareness leads to different social behaviour and thus, different infection rates. Therefore, the vigilant (V) compartment added, which represents the people that are aware. These compartments are assigned to nodes in random directed graphs to study the network dynamics. The stability properties for both homo- and heterogeneous infection parameters are found. Later, Nowzari et al. (2015) applies mean-field approximation to obtain ODE's describing its dynamics. These ODE's are used to solve several optimal control problems. Figure 2.6 shows the compartment and its interrelations on the left side and the corresponding differential equations on the right side.

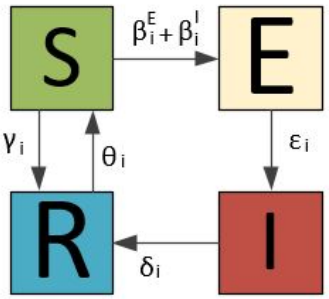

$$\begin{aligned}
S_i(t) &= 1 - E_i(t) - I_i(t) - V_i(t) \\
\dot{E}_i(t) &= (1 - E_i(t) - I_i(t) - V_i(t)) \left(\sum_{j \in \mathcal{N}_i^{\text{in}}} \beta_E E_j(t) + \beta_I I_j(t) \right) - \varepsilon E_i(t) \\
\dot{I}_i(t) &\varepsilon E_i(t) - \delta I_i(t) \\
\dot{V}_i(t) &= \delta I_i(t) + \theta\,(1 - E_i(t) - I_i(t) - V_i(t)) - \gamma V_i(t)
\end{aligned} \qquad (2.16)$$

Figure 2.6: Schematic representation of the G-SEIV model. Showing the compartments and its interrelations on the left and the corresponding differential equations on the right.

2.3 Metapopulation models

A downside of network models are that it is very hard to model every single individual in a population separately and it would take a lot of computing power Duan et al. (2015). To overcome this, metapopulation models are created. Metapopulation models are network models where every node represents a subpopulation (such as a city or a county) instead of an individual. Within each subpopulation the dynamics are homogeneous. The benefits of metapopulation are that it can easily capture heterogeneous dynamics. This can ultimately be used to study localized control intervention policies.

2.3.1 Metapopulation SIS model

Lajmanovich and Yorke (1976) created one of the first metapopulation models to study the evolution of Gonorrhea. The disease Gonorrhea doesn't lead to immunity, and therefore, they only used the S, and I state. A metapopulation model is used because there is a big difference in the infection rates between sub-populations. They proposed 8 different sub-populations based

on gender and sexual activity. The resulting model is described by equation (2.17), where L_{ij} denotes the contact matrix, N_i the size of the sub-populations, $I_i(t)$ the fraction of infected at time t, and $1/D_i$ the chance of an infective recovering.

$$\frac{d\left(N_i I_i\right)}{dt} = \sum_{j=1}^{8} L_{ij}\left(1 - I_i\right) N_j I_j \quad - \quad \frac{N_i I_i}{D_i} \tag{2.17}$$

They studied threshold conditions to reach different equilibria and the stability properties of those equilibria.

2.3.2 Homogeneous metapopulation SIR model

Hethcote (1978) made a metapopulation version of the SIR model, to study the effect of immunization on network models. The metapopulation SIR model divides the population into N groups (denoted by i). These groups can either be in the S, I or R state. The dynamics of the network SIR model is shown (2.18)

$$\begin{aligned} \dot{S}_i(t) &= -\beta s_i(t) \sum_{j=1}^{n} a_{ij} i_j(t) \\ \dot{I}_i(t) &= \beta s_i(t) \sum_{j=1}^{n} a_{ij} i_j(t) - \gamma i_i(t) \\ \dot{R}_i(t) &= \gamma i_i(t) \end{aligned} \tag{2.18}$$

Here, β is the infection rate, γ the curing rate and a_{ij} represents the adjacency matrix. As can be seen, the infection rate β and the curing rate γ are homogeneous for all nodes. However, in contrast to the population SIR model, the state change of a node depends on its neighbours. The dynamics show that the infection rate is proportional to the number of infected neighbours. Mei et al. (2017) analyzed the properties of these dynamics. They found that the effective reproduction number is $R(t) = \beta\lambda_{\max}(t)/\gamma$, where $_{\max}$ represents the dominant eigenvalue of the adjacency matrix. When $R(t) > 1$, an epidemic outbreak occurs, and when $R(t) < 1$, the infection will die out exponentially fast.

2.3.3 Heterogeneous metapopulation SIR model

Mendoza (2020) constructed a heterogeneous metapopulation SIR model. In this model, each subpopulation has a time-dependent transmission rate. These transmission rates depend on the subpopulations' onset times (time when the first infection arose) and the exchange of individuals in between the subpopulations. In contrast to previous studies, the heterogeneous infection rates are introduced internally by a dynamical equation. The resulting system of equations are described by equation (2.19).

$$\begin{aligned}
\frac{ds_i}{dt} &= -s_i(t)\frac{1}{n}\sum_{j=1}^{n}\beta_{ij}i_j(t) \\
\frac{di_i}{dt} &= s_i(t)\frac{1}{n}\sum_{j=1}^{n}\beta_{ij}i_j(t) - \gamma i_i(t), \\
\frac{dr_i}{dt} &= \gamma i_i(t)
\end{aligned} \tag{2.19}$$

Where i represents the subpopulation and the other variable represent the usual network SIR parameters. As can be seen, the curing rate γ is chosen to be the same over all the subpopluations. The infectious rate β_{ij} is described by

$$\beta(t) = \beta_0 \frac{s_{eff}(t)}{s(t)}$$

Where $s_{eff}(t)$ is described by,

$$s_{eff}(t) \equiv \sum_{i=1}^{n} s_i\left(t - t_i\right)\left[\frac{\frac{1}{n}\sum_{j=1}^{n}\beta_{ij}\left(t_i, t_j\right) i_j\left(t - t_j\right)}{n\beta_0 i(t)}\right]$$

This equation shows how the onset time $s_i\left(t - t_i\right)$ and the internal infection rate $\beta_{ij}\left(t_i, t_j\right)$ relate to the effective infection rate. After comparing the model to real data, they found that this model can accurately predict the behaviour of COVID-19. After analyzing this model, several conclusions are drawn. A larger dispersion in onset times (asynchronicity) leads to a higher delay of propagation and on the long term lead to less infected individuals. Another conclusion that is taken is that more asynchronization lead to a less probability of infections. In the real-world, this means that imposing travel restriction and partially isolating subpopulations enhances the mitigation of the virus.

2.3.4 Metapopulation SIS model

Sattenspiel et al. (1995) Argues that travel between different regions has a high impact on the spreading of the disease. Therefore, he proposes one of the first heterogeneous metapopulation models. The biggest contribution of this model is that travel between locations is incorporated in the existing SIR model. Two case studies are presented to validate this model. Later, Arino and Van den Driessche (2003) applied this theory on a SIS model. In addition, they added the effect of deaths and births to the model while keeping a constant population. They studied the stability of the equilibria and derived the expression to calculate the reproduction number R_0. The dynamics of the SIS metapopulation model is described by (2.20)

$$\begin{aligned}
\frac{dS_{ii}}{dt} &= \sum_{k=1}^{n} r_{ik}S_{ik} - g_i S_{ii} - \sum_{k=1}^{n}\kappa_i\beta_{iki}\frac{S_{ii}I_{ki}}{N_i^p} + d\left(N_i^r - S_{ii}\right) + \gamma I_{ii} \\
\frac{dI_{ii}}{dt} &= \sum_{k=1}^{n} r_{ik}I_{ik} - g_i I_{ii} + \sum_{k=1}^{n}\kappa_i\beta_{iki}\frac{S_{ii}I_{ki}}{N_i^p} - (\gamma + d)I_{ii}
\end{aligned} \tag{2.20}$$

Where S_{ij} and I_{ij} denote the number of susceptible and infected individuals from city i who are present in cities j.$\beta_{ikj} > 0$ denotes the transmission of the proportion of contacts in city j between a susceptible from city i, j, k. $\kappa_j > 0$ is the average number of contacts in city j. γ denote the recovery rate. As can be seen from the dynamics, the recovery rate is assumed

to be the same for each population. Shen et al. (2012) argues that the curing rate differs per region. Therefore, they made an extended model with a curing rate depending on the indegree of each node (k). This model is then be used to study the effect of proper distributing of medical resources. It is found that nodes with high degree (big cities) should be allocated more resources. The optimal resources allocation of a node is proportional to $k^{1.3}$

2.3.5 Metapopulation SEIIR model

Birge et al. (2020) studies the optimal economical control of different regions in New York City. A heterogeneous metapopulation (in this paper described as "spatial") model was created. In this model every region in NYC has its own SEIIR dynamics. The SEIIR compartments represent susceptible (S), exposed (E), Infected symptomatic (I), Infected asymptomatic or sub-clinical (I) and recovered (R). The compartments and their interrelations are shown in figure 2.7 and the corresponding differential equations in appendix A. The Infected are split into two separate compartments because they expect that subclinical patients have a lower infection rate. The compartments of each node, together with the graph, create the dynamics of NYC. Here it is assumed that the control parameter is a number between 0 and 1 which represents the economic activity of each region.

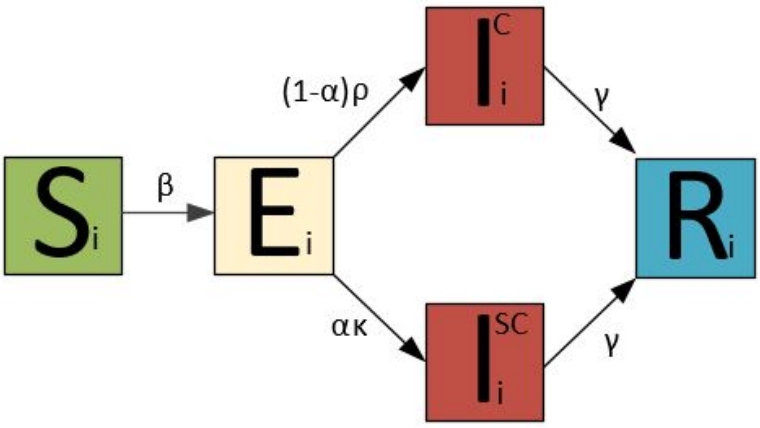

Figure 2.7: Schematic representation of the SEIRR model. Showing the compartments and its interrelations.

After that, this model is used to determine the optimal economic activity level per region. Optimal control is considered to maximize economic activity while decreasing infections. They found that by closing targeted regions, the maximum efficiency can be achieved. Moreover, they found that not necessary the region with the highest infections should be closed. Some regions with a higher economic value should have a higher closing threshold. Meaning that it can be possible to shut the surrounding regions is preferable.

2.3.6 Metapopulation SIQHDR model

Della Rossa et al. (2020) made a heterogeneous metapopulation model of Italy, to study the effect of regional differences during the COVID-19 pandemic. The nodes in this metapopulation model represent twenty different regions in Italy. The dynamics of each node is described by six compartments, which are susceptible (S_i), infected (I_i), quarantined (Q_i), hospitalized (H_i), recovered (R_i) and deceased (D_i) are. figure 2.8 shows the graph of the network (left) and the relationship between the compartments (right). The corresponding differential equations can be found in appendix A.

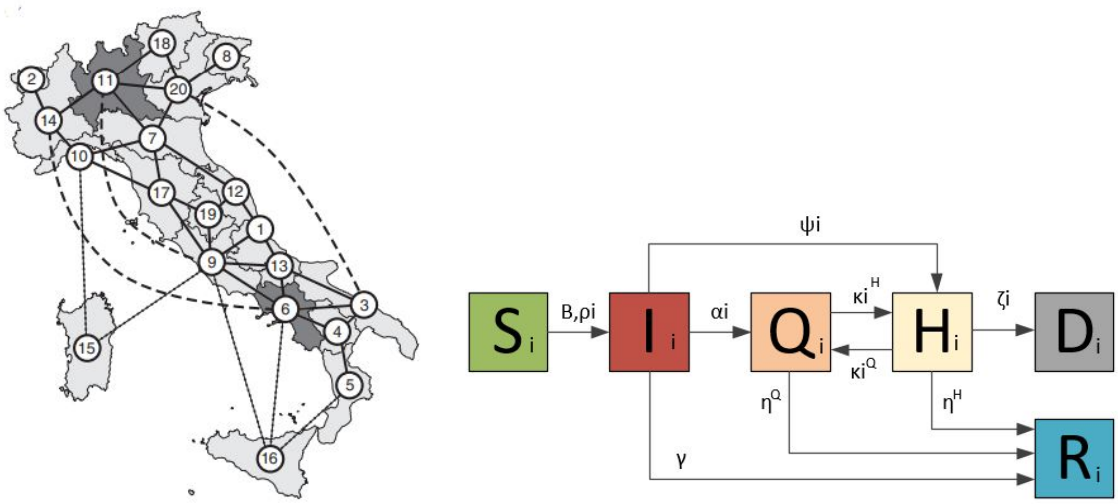

Figure 2.8: Schematic representation of the SIHQDR model. Showing it's compartments and their interrelations on the right and the topology on the left

This model is used to study 1) the effect of heterogeneity in between the regions 2) the effects of the flows across regions 3) differentiated region-specific interventions strategies. Using this model, they acknowledge found that heterogeneity between regions matter. Moreover, they found that when only one region relaxes its containment measures, the disease will still spread to the closed regions. Moreover, they constructed a differentiated feed-back strategy. This strategy holds that every region takes containment measures based on infected individuals and hospitalized patients. Above all, they found that the effects on the total number of infected will be almost the same as a nationwide lock-down strategy, while it mitigates the economic costs.

2.3.7 Metapopulation SHARUCD model

Aguiar et al. (2020) studied the COVID-19 infections in the Basque Country. Their goal was to make a model which can help healthcare authorities and the government with predictions in amount of infections, ICU admissions, hospitalizations, and deceased cases. To reach this goal they made the SHARUCD model, which compartments are Susceptible (S), hospitalization (H), Asymptomatic or sub-clinical (A), Recovered (R), patient on the intensive care (U), cumulative recorded cases (C), and deceased (D).

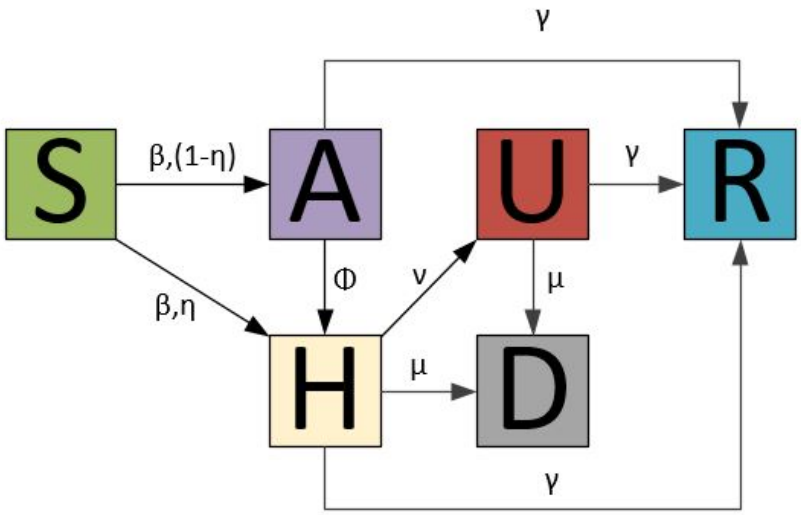

Figure 2.9: Schematic representation of the SHARUCD model. Showing the compartments and its interrelations.

This model makes a clear distinction between hospitalized individuals and sub-clinical individuals to make accurate predictions on health care necessities. Moreover, this is a stochastic model and it's deterministic approximations leads the differential equations described in appendix A. An interesting refinement in this model was that it synchronizes the ICU admission on hospitalizations instead of deceased or recovered. This refined model was then used to accurately make short and mid-term predictions.

2.3.8 Metapopulation SEPIAHQRD model

Gatto et al. (2020) met a metapopulation model, where each node represents a region in Italy. The dynamics of each region is described by the SEPIAHQRD dynamics, which exists of the following compartments: Susceptible (5), Exposed (E), Presymptomatic (P) Infected with heavy symptoms (I), Asymptomatic/mildly symptomatic (A), Hospitalized (H), Quarantined at home (Q), Recovered (R), and Dead.

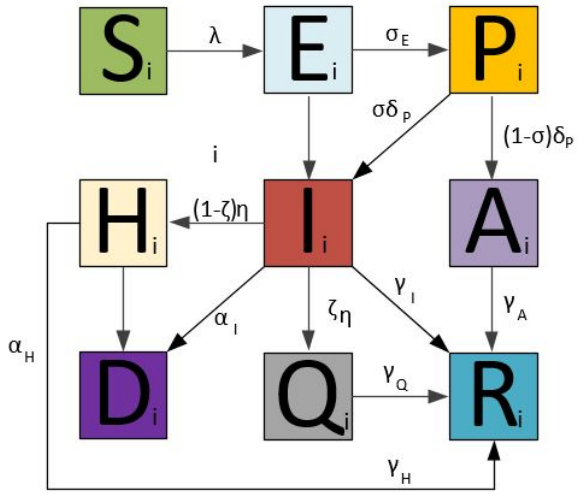

$$
\begin{aligned}
\dot{S} &= -\lambda S \\
\dot{E} &= \lambda S - \delta_E E \\
\dot{P} &= \delta_E E - \delta_P P \\
\dot{I} &= \sigma\delta_P P \\
&\quad - (\eta + \gamma_I + \alpha_I)\, I \\
\dot{A} &= (1-\sigma)\delta_P P - \gamma_A A \\
\dot{H} &= (1-\zeta)\eta I - (\gamma_H + \alpha_H)\, H \\
\dot{Q} &= \zeta\eta I - \gamma_Q Q \\
\dot{R} &= \gamma_l I + \gamma_A A + \gamma_H H \\
\dot{D} &= \alpha_l I + \alpha_H H
\end{aligned}
\tag{2.21}
$$

Figure 2.10: Schematic representation of the SEPIAHQRD model. Showing the compartments and its interrelations on the left and the corresponding differential equations on the right

The goal of this model is to test the effects of localized containment measures and travel restrictions. The papers uses this model to evaluate the effects of the measures taken by the government in march 2020. It is estimated that the measures reduced transmission by 45 %. This results in a total amount of averted hospital cases of 733.000 individuals at the end of march. Moreover, this paper shows that the presymptomatic patients significantly contribute to the spreading of the disease. this implies that massive testing can contribute to the containment of the disease.

2.4 Overview of the models

In table 2.1, an overview of the models are listed. For every model, the variant, type, stochasticity, and the contribution of its corresponding paper is described. The variant lists the altered versions of the corresponding compartment model. The type is divided into population, network and metapopulation. 'Population' is assigned to the papers that consider the population as a whole, resulting in much heterogeneity. 'Network' is assigned to papers that consider every individual separately as a node in a graph. 'Metapopulation' is assigned when every node represents a small subpopulation instead of an individual. The fourth column distinguishes between deterministic or stochastic. In deterministic models, infections happen at a specific rate while stochastic models assume a probability for every individual to get infected (Nowzari et al., 2016). The last column describes the contribution of the paper.

Comparison				
Model	**Variation**	**Type**	**Deterministic/ Stochastic**	**Papers contribution**
SIR	Kermack and McKendrick (1927)	Population	Deterministic	First spreading disease model
	Xia et al. (2012)	Network	Deterministic	New SIR network model containing the infection delay property of a virus
	Mei et al. (2017)	Network	Deterministic	Analytical results for transient behavior, threshold conditions, stability properties, and asymptotic convergence
	Hethcote (1978)	Metapopulation	Deterministic	A homogeneous metapopulation SIR model
	Mendoza (2020)	Metapopulation	Deterministic	A heterogeneous infection rate dependent on time
SIS	Kephart and White (1992)	Network	Deterministic	Constructed a network SIS model
	Wang et al. (2003)	Network	Stochastic	Studied the properties of the discrete-time SIS model
	Van Mieghem et al. (2008)	Network	Stochastic	Studied the properties of the continuous-time SIS model
	Gross et al. (2006)	Network	Stochastic and Deterministic	Showing effects of changing topologies
	Lajmanovich and Yorke (1976)	Metapopulation	Deterministic	First SIS metapopulation model to study Gonorrhea
	Shen et al. (2012)	Metapopulation	Stochastic	Using a heterogeneous curing rate, optimal medical distribution is found
SEIR/ SEIRS	Hethcote and Van den Driessche (1991)	Population	Deterministic	Modeled the incubation period of a disease
	Li and Muldowney (1995)	Population	Deterministic	Found the stability properties of the SEIR/-SEIRS model
	Li et al. (1999)	Population	Deterministic	Modeled a varying population size
G-SEIV	Nowzari et al. (2014)	Network	Stochastic	Providing a generalized network model

	Nowzari et al. (2015)	Network	Stochastic / deterministic	Providing a deterministic G-SEIV model and study optimal control problems
SEIIR	Birge et al. (2020)	Metapopulation	Deterministic	Showing the effects of region targeted control measures
SIQHDR	Della Rossa et al. (2020)	Metapopulation	Deterministic	Proposing a optimal differentiated feedback control strategy for fighting COVID-19 in Italy
SEAIRD	Djidjou Demasse et al. (2020)	Population	Deterministic	Showing the optimal control intensity on infection rate until vaccine development
SHARUCD	Aguiar et al. (2020)	Population	Stochastic	Accurate short and mid-term predictions for the basque country in the number of infections, ICU admissions, hospitalizations, and deceased cases
SIDARTHE	Giordano et al. (2020)	Population	Deterministic	Discriminates between detected and undetected infected and sheds light on the effects of contact tracing
SEPIAHQRD	Gatto et al. (2020)	Metapopulation	Stochastic	Showing the effects of localized containment measures in Italy

Table 2.1: Overview reports

2.5 Conclusion

Out of this literature review, it became clear that the decision of a spreading disease model highly depends on the research question. For this research, the following decisions are made:

- It is chosen to design a metapopulation model over an agent-based model. The reason for this is that population models become accurate when the population size is large enough. The randomness of disease is then simplified to certain rates.
- The model will have six compartments, namely: Susceptible (S), Infected undetected (I), Infected Detected (D), Infected Acutely Symptomatic (A), recovered (R), Extinct (E). Splitting the infected into three different compartments is needed due to their different infection rates. More compartments would lead to more unnecessary complexity.

Chapter 3: Design of the SIDARE model

In this chapter, the design of the metapopulation SIDARE model is discussed. First, the SIDARE compartments and its corresponding dynamics are explained. After that, The chosen parameters are shown and justified. Finally, the model's accuracy is validated in by comparing the outcomes to an earlier done research.

3.1 SIDARE model formulation

The metapopulation SIDARE model will be an extended version of the population SIDARE model (Andreas Kasis, 2021). The scope of this research is to take the Netherlands as population. The Netherlands has a large population of around 17 million; thus, a deterministic approach will suffice. The SIDARE model divides the population into six compartments, namely: Susceptible (S), Infected Undetected (I), Infected Detected (D), Infected Acutely Symptomatic (A), Recovered (R), Extinct (E). The population is assumed to be constant so at any time t : $S(t) + I(t) + D(t) + A(t) + R(t) + E(t) = N(t)$, Where $N(t)$ is equal to the population size of the Netherlands.

At the beginning of the pandemic, individuals are classified as susceptible and get infected through contacts with Infected with rate β. After that, a proportion of the infected progresses to $D(t)$ with testing rate ν or to $A(t)$ with severity rate ξ_i. The Recovered compartment increases with rate $\gamma_i, \gamma_d, \gamma_a$ from the compartments $A(t), D(t), I(t)$ respectively. The amount of extinct is proportional to the amount of Acutely Symptomatic with death rate μ. The resulting differential equations are shown in equation (3.1)

$$\dot{S} = -\beta si \tag{3.1a}$$
$$\dot{I} = \beta si - \gamma_i i - \xi_i i - \nu i \tag{3.1b}$$
$$\dot{D} = \nu i - \gamma_d d - \xi_d d \tag{3.1c}$$
$$\dot{A} = \xi_i i + \xi_d d - \gamma_a a - \mu a \tag{3.1d}$$
$$\dot{R} = \gamma_i i + \gamma_d d + \gamma_a a \tag{3.1e}$$
$$\dot{E} = \mu a \tag{3.1f}$$

In the metapopulation SIDARE model, every province in the Netherlands has its own local SIDARE dynamics. This means that a total of $6 * 12 = 72$ differential equations describe the COVID-19 dynamics in the Netherlands. These sets of differential equations are linked by a ϕ matrix that represents the travel between them. Figure 3.3 Shows the compartments including its interrelations on the left and the topology on the right. As can be seen from the figure, the graph's nodes represent the different provinces in the Netherlands. The link between them shows the fluxes of people that move between the provinces on a daily bases. For clarity, only the neighbouring provinces are shown in this figure. In reality, there is a link between all the provinces.

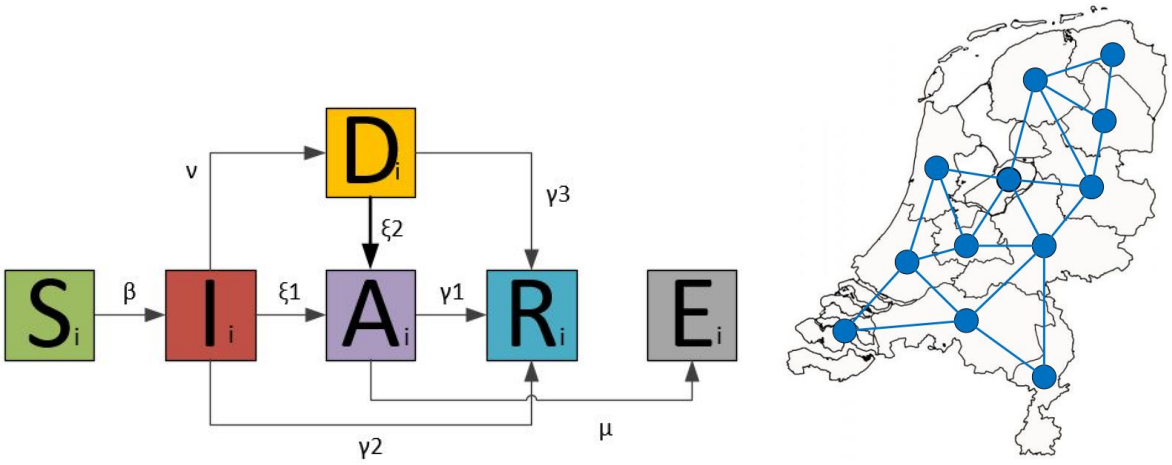

Figure 3.1: Schematic representation of the metapopulation SIDARE model, used to describe the evolution of the COVID-19 pandemic. On the left, the compartments and its' interrelation are shown. The right figure shows the topology of the metapopulation network. A link is drawn between all the neighbouring regions while in reality there is a link between all the regions.

In figure 3.3, every compartments contain an subtext i representing the different regions. Moreover, the $\xi_d, \xi_i, \gamma_a, \gamma_i, \gamma_d$, are changed to $\xi_1, \xi_2, \gamma_1, \gamma_2, \gamma_3$ respectively. The reason for this change is to avoid confusion about the meaning of the subtext i. The resulting system of differential equations is given by equation (3.2)

$$\dot{S}_i = -\sum_{j=1}^{M}\sum_{k=1}^{M} \beta \phi_{ij} S_i \frac{\phi_{kj} I_k}{N_j} \tag{3.2a}$$

$$\dot{I}_i = \sum_{j=1}^{M}\sum_{k=1}^{M} \beta \phi_{ij} S_i \frac{\phi_{kj} I_k}{N_j} - \gamma_2 I - \xi_2 I - \nu I \tag{3.2b}$$

$$\dot{D}_i = \nu i - \gamma_3 D - \xi_1 D \tag{3.2c}$$

$$\dot{A}_i = \xi_2 I + \xi_1 D - \gamma_1 A - \bar{\mu}(A) \tag{3.2d}$$

$$\dot{R}_i = \gamma_2 I + \gamma_3 D + \gamma_1 A \tag{3.2e}$$

$$\dot{E}_i = \bar{\mu}(A) \tag{3.2f}$$

Where $S_i, I_i, D_i, A_i, R_i, E_i \in (0,1) \subset \mathbb{R}^n$ represents the amount of Susceptible, Infected Undetected, Infected Detected, Recovered, Acutely Symptomatic, Extinct respectively for region i. The model parameters are described as follow:

- $\phi_{ij} \in \mathbb{R}^{n \times n}$ is a matrix where each entry denotes the percentage of people travelling between regions (flux). More specifically, this matrix denotes the ratio of people from region i (rows) that move to region j (columns). This is a normalized matrix, meaning that the sum of each row is equal to 1 $\sum_j \phi_{ij} = 1$. Similarly, ϕ_{kj} denotes the ratio of people coming from region k that interact with region j.
- $\beta \in \mathbb{R}$ denotes the rate at which susceptible get infected
- $N_j \in \mathbb{N}$ denotes the total inhabitants of region j that are able to move (Susceptible + Infected undetected + Recovered).
- $\nu \in \mathbb{R}$ denotes the detection rate of individuals
- $\gamma_1, \gamma_2, \gamma_3 \in \mathbb{R}$ denotes the recovery rate of Acutely Symptomatic, Infected and Infected Detected respectively.

- $\xi_1, \xi_2 \in \mathbb{R}$ denotes the rate of becoming Acutely Symptomatic from Infected and Infected Detected respectively.
- $\bar{\mu} \in \mathbb{R}$ denotes the rate of deceased which is explained in section 3.1.1. This rate doesn't include the natural death rate.

3.1.1 Mortality rate

The mortality rate highly depends on the healthcare capacity. If the healthcare capacity is exceeded, Acutely Symptomatic individuals are more likely to die. Therefore, the equation (3.3) is set up. This equation shows that when the amount of Acutely Symptomatic is smaller than the healthcare capacity ($a < \bar{h}$), the mortality rate is set to a constant rate μ. However, if the healthcare capacity is exceeded ($a > \bar{h}$), the mortality rate increases. Equation (3.3) shows that mortality rate stays the same for the people that get the usual care ($\mu\bar{h}$), and the mortality rate for the others changes to $\hat{u}$. The mortality rate $\hat{u}$ will be larger than μ. In this case, it is assumed that the hospital capacity stays constant.

$$\bar{\mu}(a) = \begin{cases} \mu a, \text{ if } a \leq \bar{h}, \\ \mu\bar{h} + \hat{\mu}(a - \bar{h}), \text{ if } a > \bar{h}, \end{cases} \tag{3.3}$$

3.2 Parameter values identification

In this section, the input parameter values are determined. The parameter values are based on earlier done research and current COVID-19 data. The data that is selected is from the start of the outbreak in the Netherlands, march 2020, till end of December 2020. To get a realistic model of the Netherlands, data of the Netherlands is used as much as possible. If there is no data available of the Netherlands, logical assumptions are made. A summary of the chosen parameter values can be found in table 3.1. The rest of the section is used to explain how these values are determined.

Table 3.1: Summary of the parameter values used in the metapopulation SIDARE model

Parameter	**Value**	**Justification**
β	0.171, 0.2	Section 3.2.1
γ_1	(1/14)	WHO (2020c)
γ_2	(1/14)	WHO (2020c)
γ_3	(1/12.1)	WHO (2020c)
ϵ_1	0.005	Verity et al. (2020)
ϵ_2	0.005	Verity et al. (2020)
ν	0.05	Assumed, Andreas Kasis (2021)
μ	0.0062	(health agency of sweden, 2020),Perez-Saez et al. (2020)
$\hat{\mu}$	5*μ	Assumed, Andreas Kasis (2021)
ϕ_{ij}	Section 3.2.3	Section 3.2.3

The total inhabitants of the Netherlands in 2018 was 17.181.084. (CBS, 2018). The curing rates γ_1,γ_2,γ_3 are the inverse of the average amount of days it takes for a person to recover. For infected and infected detected, this is 14 days, and for acutely symptomatic 12.1 days (WHO, 2020c). The true mortality rate of a disease is hard to estimate. The mortality rate depends on the patient's health condition and the quality of healthcare given to the patient. A common

method to describe the severity of diseases is through the Infection Fatality Ratio. The estimates of the IFR vary. A study conducted in Zwitserland reported an IFR of 0.64% (Perez-Saez et al., 2020) and a study conducted in Sweden reported an IFR of 0.6% (health agency of sweden, 2020) to 0.6 %. Therefore an average of 0.0062 is assumed.

3.2.1 Infection rate

The literature often gives different estimations of the initial reproduction number R_0.(Billah et al., 2020). Also, the reproduction number changes when NPIs are enforced. Therefore, two β values calculated 1) The initial infection rate when no measures are taken and 2) The infection rate where NPIs are taken.

1) The initial β is estimated using the initial reproduction number R_0 of 2.64 in the Netherlands (Max Roser and Hasell, 2020). The β is then calculated with the formula $\bar{R}_0 = \beta s_0 / (\gamma_i + \xi_i + \nu)$ assumed that the initial $\nu = 0$ at $t = 0$. This results in a $\beta = 0.2$

2) The infection rate can change when the government takes NPI's such as social distancing, the closing of public places, and a lockdown. These NPI's are often taken simultaneously, so it is hard to estimate the β of each NPI independently. Therefore, a β is calculated at a time where multiple NPI's are active simultaneously. The β is calculated through "parameter fitting". Parameter fitting is a technique which compares the modelling outcome to the real data. Multiple β's are taken, and the one that "fits best" is chosen. The best fit is evaluated by the least-squares method. The least-squares method minimizes the sum of the differences between the actual data and the model. The parameter estimation is applied from the beginning of June till October the 13Th. Some of the NPI's active at that time were (Rijksoverheid, 2021b):

- Social distancing of 1.5 meter
- Maximum gathering of 30 people
- The catering industry has limited opening times
- Travelers by public transport are obligated to wear a mouth mask

On October the 13th, stricter lockdown measures were taken by the dutch government. The estimated β obtained by parameter fitting is 0.172. The real data and the model estimation is shown in figure 3.2. Note that this β is only a snapshot of the actual continuously changing β.

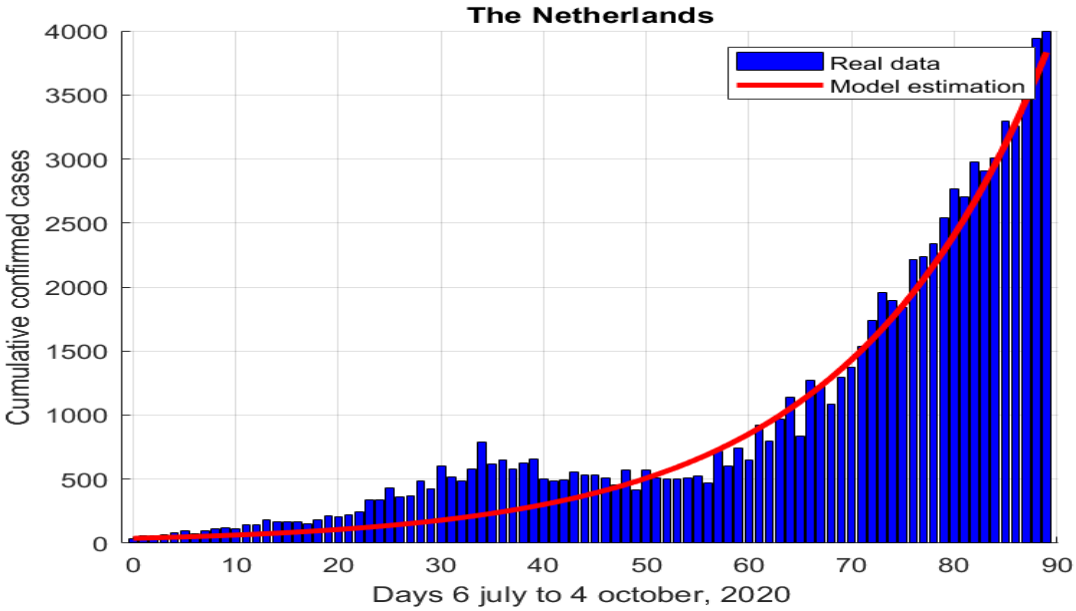

Figure 3.2: Cumulative amount of infected cases from the beginning of July till October 6th. The blue bars show the real data found at (Max Roser and Hasell, 2020), and the red line shows the model's estimation

3.2.2 Hospitalization rate

The hospitalization rate ϵ_1 and ϵ_1 are calculated by comparing the proportion of infected that are hospitalized (Verity et al., 2020) with the population of the Netherlands per age group (Nations, 2020). This data is shown in 3.2. The total amount of hospitalized divided by the total inhabitants of the Netherlands is $1031,08/17062 = 0.06$. 0.06 divided by the average length of COVID-19 (Approximately 12 days) results in a ϵ_1 and ϵ_2 of 0.005.

Table 3.2: Calculation of the hospitalization rate ϵ_1 and ϵ_2

Age	Amount (*1000)	Proportion hospitalized	Hospitalized (*1000)
0-9	1777	0	0
10-19	1990	0,04	0,81
20-29	2117	1,04	22,02
30-39	2053	3,43	70,42
40-49	2260	4,25	96,05
50-59	2506	8,16	204,49
60-69	2099	11,80	247,68
70-79	1457	16,60	241,86
>80	803	18,40	147,75
Sum	17062		1031,08

3.2.3 ϕ_{ij} matrix

To estimate the ϕ_{ij} matrix, commuting data is used. This method is consistent with the research of Della Rossa et al. (2020). The commuting data can be extracted from statline CBS (2018). this data set contains information on how many people living in province i have a job in province j. The data set is shown in table 3.3.

Table 3.3: Data retrieved from CBS (2018) showing the amount of commuting between the 12 provinces of the Netherlands $*10^{-3}$. The rows denotes the home region and the corresponding columns denote the where those people work

	Groningen	Friesland	Drenthe	Overijssel	Flevoland	Gelderland	Utrecht	Noord-Holland	Zuid-Holland	Zeeland	Noord-Brabant	Limburg
Groningen	524,9	10,9	27,9	5,3	1,4	2,5	1,9	3,3	2,6	0	2	0,2
Friesland	17,5	594	8,1	6,6	4	3,1	2,2	5,4	3,5	0,1	2,5	0,2
Drenthe	30,1	4,9	413,9	28,1	1,7	4,6	1,8	2,4	2,2	0	2	0,4
Overijssel	2,4	3	13,5	1044,3	14,8	47,8	7	6,4	4,8	0,1	5,5	1,9
Flevoland	0,5	1,4	0,8	10,9	307,5	25,8	9,6	45,2	4,3	0,1	3,6	1,9
Gelderland	1,1	1,4	2,1	42,4	11,2	1808,3	62,3	24	22,8	0,7	49	34,8
Utrecht	0,6	0,5	0,7	3,9	4,4	34,7	1087,2	103,8	43,1	0,4	13,6	2,5
Noord-Holland	1,3	1,5	1,2	4,3	10,1	10,6	60,6	2672,7	51,9	0,5	14,1	2,3
Zuid-Holland	0,1	0,1	0	0,3	0,1	1,1	1,6	1,7	3535,3	126,7	13,7	0,3
Zeeland	0,2	0,2	0,1	0,4	0,2	0,7	1,7	1,9	10,1	356,504	9,9	0,4
Noord-Brabant	0,8	0,4	0,7	4,8	1,3	34,2	22,4	17,5	78,6	14,8	2324,286	28,5
Limburg	0,2	0,1	0,4	1,6	0,4	14,1	3,7	4,6	9	0,5	66,9	1015,698

Commuting data is believed to give a good approximation of the travel between provinces. To get to a realistic normalized ϕ_{ij} matrix, some operations have to be done. Firstly, the people that don't work have to be taken into account. These will be added on the diagonals, meaning that it is assumed that they don't travel on a daily bases. Secondly, not everyone travels to work. It is assumed that 10 % of the people work at home on a daily bases. Thereby, in the Netherlands, it is common to have five working days a week. These values are multiplied to the number of people that work in another region. Finally, the matrix is normalized such that the sum of each row is equal to one. The resulting ϕ_{ij} matrix is sown in table 3.4.

Table 3.4: ϕ matrix shows the percentage of the people who live in one region and work in another region based on commuting data. The rows denote the home region, and the corresponding columns denote the where those people work. The calculation of this matrix can be found in chapter E line 20-33

	Groningen	Friesland	Drenthe	Overijssel	Flevoland	Gelderland	Utrecht	Noord-Holland	Zuid-Holland	Zeeland	Noord-Brabant	Limburg
Groningen	0,94	0,01	0,03	0,01	0,00	0,00	0,00	0,00	0,00	0,00	0,00	0,00
Friesland	0,02	0,95	0,01	0,01	0,00	0,00	0,00	0,01	0,00	0,00	0,00	0,00
Drenthe	0,04	0,01	0,90	0,04	0,00	0,01	0,00	0,00	0,00	0,00	0,00	0,00
Overijssel	0,00	0,00	0,01	0,94	0,01	0,03	0,00	0,00	0,00	0,00	0,00	0,00
Flevoland	0,00	0,00	0,00	0,02	0,84	0,04	0,01	0,07	0,01	0,00	0,01	0,00
Gelderland	0,00	0,00	0,00	0,01	0,00	0,92	0,02	0,01	0,01	0,00	0,02	0,01
Utrecht	0,00	0,00	0,00	0,00	0,00	0,02	0,90	0,05	0,02	0,00	0,01	0,00
Noord-Holland	0,00	0,00	0,00	0,00	0,00	0,00	0,01	0,96	0,01	0,00	0,00	0,00
Zuid-Holland	0,00	0,00	0,00	0,00	0,00	0,00	0,00	0,00	0,97	0,02	0,00	0,00
Zeeland	0,00	0,00	0,00	0,00	0,00	0,00	0,00	0,00	0,02	0,96	0,02	0,00
Noord-Brabant	0,00	0,00	0,00	0,00	0,00	0,01	0,01	0,00	0,02	0,00	0,95	0,01
Limburg	0,00	0,00	0,00	0,00	0,00	0,01	0,00	0,00	0,01	0,00	0,04	0,94

3.3 Assumptions SIDARE

The following assumptions are made in the metapopulation SIDARE model.

- In this model a constant population is assumed and no birth or death ratio is taken into account.
- This model assumes that the individuals in the recovered compartment will be immune to the disease.

- There is no travel modelled in or outwards the Netherlands, meaning that no infected cases are imported.
- Infected Detected and Acutely Symptomatic are assumed to not contribute to the spreading of the disease. Moreover, Acutely Symptomatic are assumed to require hospitalization
- All provinces in the Netherlands are assumed to be homogeneous. This means that all the parameters mentioned in section 3.2 will be the same for every province
- In this model the reduced traffic doesn't lead to less social interactions. In reality, it would be logical that not traveling to another province results in less contacts. Above that, the travel in this model is based on commuting data.

3.4 Travel control by changing the Phi-matrix

Travel control is modelled by changing the ϕ matrix. The new ϕ matrix is calculated by manipulating the commuting matrix and then normalize it. The formula that manipulates the commuting data is shown in equation (3.4).

$$A_{new} = A_{ij} * (1 - U) \circ (1 - Adj) + Adj \circ \left(A_{ij} + \sum_{i=1}^{12} (A_{ij} \circ (1 - Adj) * U) \right) \tag{3.4}$$

Here A_{new} denotes the new commute matrix and A_{ij} the original commuting matrix shown in table 3.3. $U \in [0, 1] \subset \mathbb{R}$ denotes the control input that is applied. The Adj denotes the adjacency matrix, which shows whether pairs of vertices are adjacent or not. The $\circ$ denotes the Hadamard product (Element-wise multiplication). The formula can be explained by an example where a nationwide travel restriction of 90% is applied. The first part of the equation $A_{ij} * (1 - U) \circ Adj$ reduces the number of commuters from the off-diagonals. So, in this case, the off diagonals will be 10% of the original commuting matrix. The second part of the formula adds the reduced commuters from the off-diagonals to the diagonals.

To obtain the resulting ϕ matrix, the commuting matrix A_{new} has to be normalized such that $\sum_j \phi_{new} = 1$. This strategy can be used to simulated the four different cases discussed in this report.

3.5 Validation of the SIDARE

To validate the SIDARE model, the model is applied to a previously done study. The research that is chosen to compare SIDARE model with is the SIDQHR Della Rossa et al. (2020). As described in section 2.3.6, this paper studies the effect of regional differences and traffic between regions in Italy during the COVID-19 pandemic. This study is chosen because they use a similar model which can describe the evolution of COVID-19 accurately. However, there is a difference between the compartments that are chosen. The compartments that overlap are susceptible, infected and extinct. It is chosen to compare the models on the infected compartment. To compare this, the relevant data of the SIDQHR is imported into the SIDARE model. By making a few changes, a figure given in the supplementary materials can be recreated.

The comparison is shown in section 3.5. The left picture shows the graph of Della Rossa et al. (2020) with only social distancing as NPI. Blue, magenta, red, green, and black solid lines correspond to the fraction of infected, quarantined, hospitalized requiring ICU, recovered, and deceased in the population (right y-axis). The right picture shows the recreated amount of infected using the SIDARE model. It can be seen that the blue line on the left image reaches the same amount of infected within the same amount of time as the left picture. The same

experiment is run on a regional level. Figure D.1 shows that the amount of infections calculated by both models are similar. It can be concluded that the SIDARE model gets the same results as the SIDQHR model.

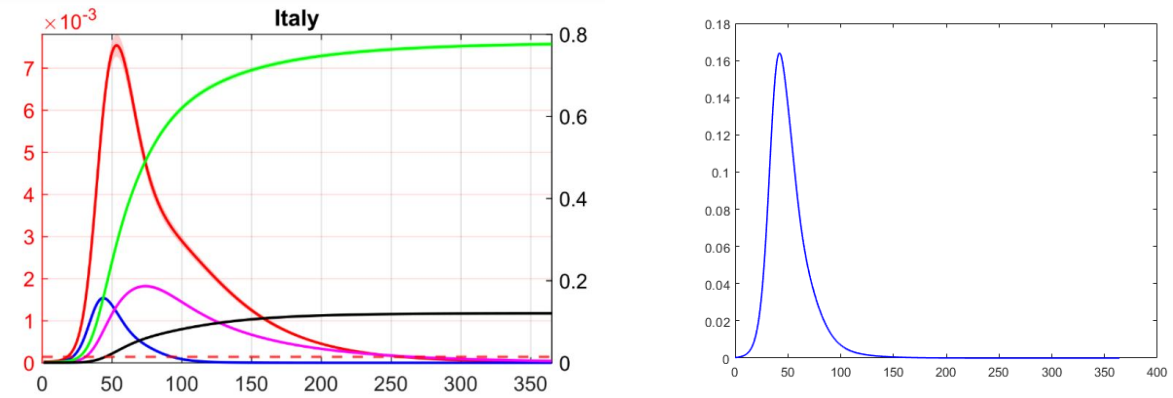

Figure 3.3: The left picture shows the graph of Della Rossa et al. (2020) with only social distancing as NPI. Blue, magenta, red, green, and black solid lines correspond to the fraction of infected, quarantined, hospitalized requiring ICU, recovered, and deceased in the population (right y-axis). The right picture shows the recreated amount of infected using the SIDARE model.

Chapter 4: Simulating travel restricting measures

In this chapter, four cases containing travel restricting measures are simulated. The goal is to investigate to what extend travel restriction measures makes sense and if so, what will be the best way to execute it. The four different cases are:

- **Case I** Nationwide travel restricting measures. In this case, every province will be isolated, meaning that only travel within each province is allowed.
- **Case II** Regional travel restricting measures. In this case, one of the provinces is isolated from the rest. This case will be repeated for every province.
- **Case III** In this case, a cut-set is used to divide the Netherlands into two clusters: the Northeast and the Southwest. Individuals are able to travel within each cluster, but not to the other cluster.
- **Case IV** Only permitting travel in a 'target' cluster. This case is the same as case III, but in this case, one of the clusters is smaller. The composition of the target cluster is now based on the amount of travel between provinces.

For every case, the effect on the timing and magnitude of the national infection peak is analyzed. Also, for the relevant cases, the effect on regional infections are analyzed. A parameter variation is applied on the β to see the effects of changing infection rates.

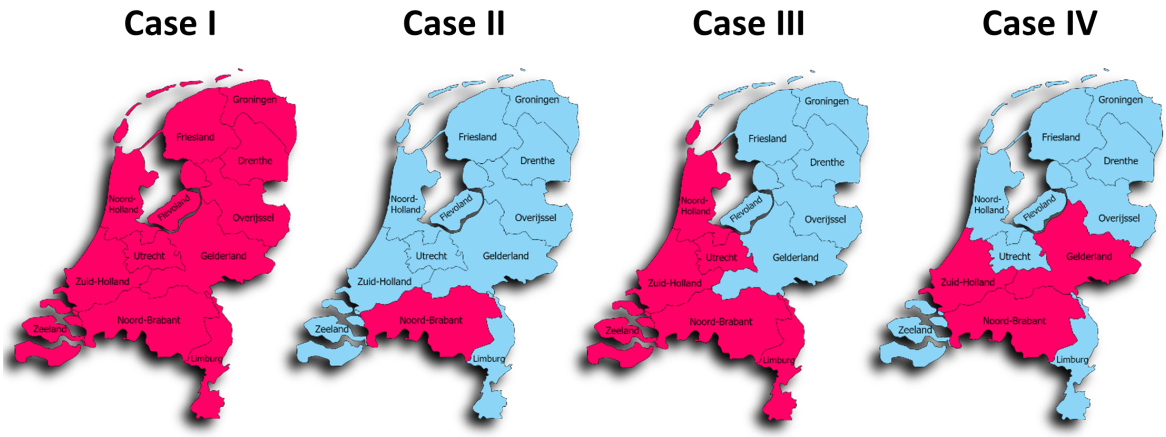

Figure 4.1: Visualization of the four different cases that are studied in this chapter

The initial conditions for every case are shown in equation (4.1). The one initial infection in I(0) represents the first detected individual in Noord-Brabant on 27th February 2020 (RIVM, 2020). The initial susceptible are each province's inhabitants ($\vec{N}$) minus the initial infections. The rest of the initial conditions are set to zero.

$$I(0) = \begin{pmatrix} 0 \\ \vdots \\ 0 \\ 1 \\ 0 \end{pmatrix} \in \mathbb{R}^{12}, \qquad S(0) = \vec{N} - I(0), \qquad D(0) = A(0) = R(0) = E(0) = \vec{0} \in \mathbb{R}^{12} \tag{4.1}$$

4.1 Case I: Nationwide travel control

Nationwide control is simulated by using equation (3.4). The adjacency matrix corresponding to can be found in appendix C. A simulation is run with a control effort from 0 to 99 %.

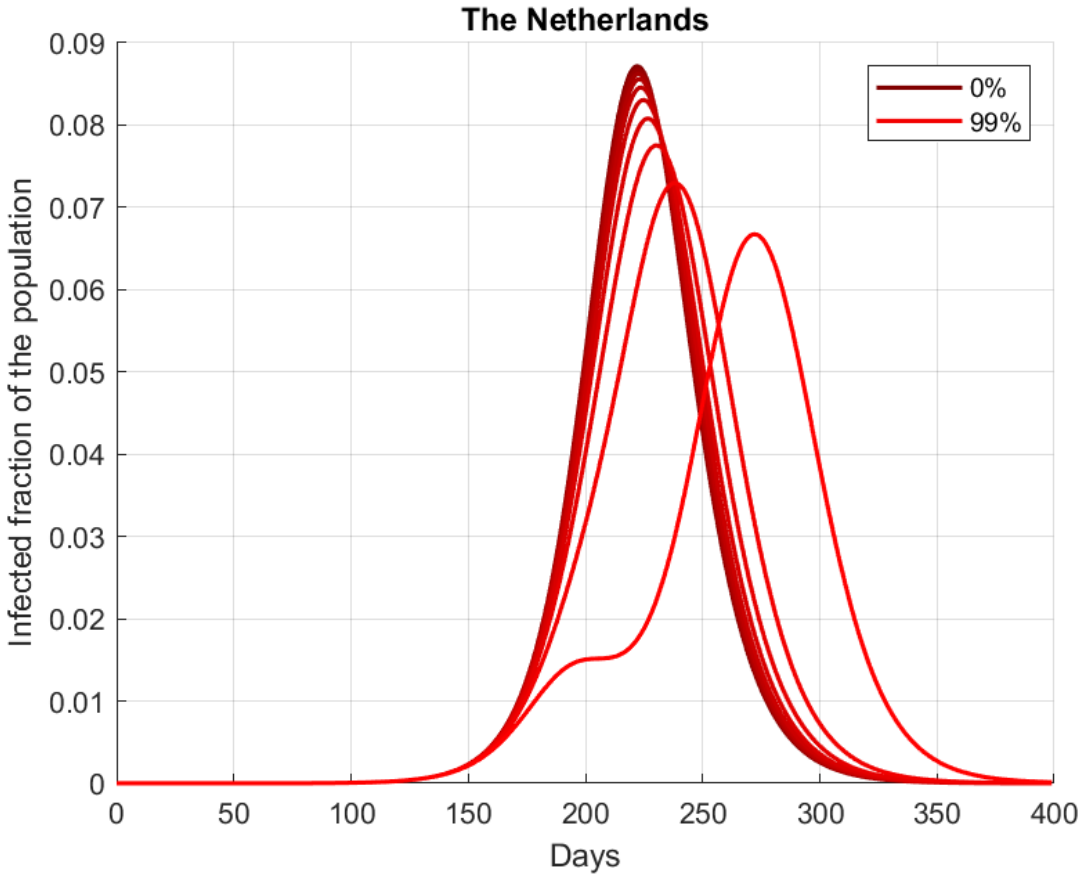

Figure 4.2: The effect of nationwide travel restrictions from 0 to 99% on the national infection peak. The lightest colour shows the highest control effort

For a $\beta = 0.2$, it is found that no matter the control effort, the total cases and total deceased will still be the same (11.5 million cases and 271.000 deaths). This can be explained due to the fact that the virus will still reach all the provinces. Within those provinces, there are no containment measures so that the equilibrium will stay the same. However, a difference can be found in the magnitude and the timing of the infection peak. These effects are visualized in figure 4.2. When no control effort is applied, the peak of infections will have a magnitude of 0.087 fractions of the population at day 210. By increasing the control effort, the magnitude can be decreased and the time of the peak delayed. When 99% control effort is applied, the peak of infections will have a magnitude of 0.067 fractions of the population at day 261—resulting in a total delay in the infection peak of 51 days and a decrease of 0.02 in magnitude. These delays are relatively low compared with the results of Della Rossa et al. (2020). This can be explained by the fact that the ϕ matrix in this research is different. In the Netherlands, an average of 5% of the people working in another province, while in Italy this is less than 1%. The high amount of travel in the Netherlands makes a higher restriction needed to achieve the same delay. The effect of nationwide travel restricting measures on the acutely symptomatic are similar to the infected. These results are plotted in figure D.2 in appendix D. The black dotted line represents the health care capacity of 337 per 100.000 inhabitants (Rhodes et al., 2012). It can be seen that

the health care capacity is greatly exceeded.

4.2 Case II: Regional travel control

In this section, regional control will be analyzed. Regional control means that only one province is isolated from the rest, so that all the in- and outgoing travel of that province is restricted. The regional control experiment is repeated twelve times such that the isolation of every province is studied. For every isolated province, the effect of the total delay and magnitude on the national infection peak will be analyzed. The results of these experiments are shown in table 4.1 and table 4.2.

Table 4.1: This table shows the effects of isolating one province on the national infection peak's delay. The columns correspond to the isolated province and the rows to the amount of control effort (0 to 99%).

Control (%)	Groningen	Friesland	Drenthe	Overijssel	Flevoland	Gelderland	Utrecht	Noord-Holland	Zuid-Holland	Zeeland	Noord-Brabant	Limburg
0-60	0	0	0	0	0	0	0	0	0	0	0-2	0
70	0	0	0	0	0	1	0	1	1	0	4	0
80	0	0	0	0	0	1	0	1	1	0	8	0
90	0	0	0	0	0	1	1	1	2	0	15	0
99	0	0	0	0	0	0	0	-2	-1	0	48	0

Table 4.1 shows the delay in the national infection peak compared when no control is applied. The delay depends on the control effort (rows) and the province to which the control effort is applied (columns). The table shows that for 0 to 60% the infection peak will have no delay. An exception can be seen in the province Noord-Braband, where the initial infections occurred. It can be concluded that isolating one province makes sense when it is the only province with infections. The peak can be delayed by 48 days. By comparing this result with the nationwide effects in section 4.1, it can be seen that controlling nationwide wins you only three days. Nationwide travel restrictions have more impact than regional travel restriction on the daily life of people. This means that regional travel restrictions are significantly more effective than nationwide travel restrictions.Table 4.2 shows that the peak of infections can be decreased to 7.4% of the population. This implies that heavy regional travel restrictions have little effect on the national infection peak.

Table 4.2: This table shows the effects of isolating one province on the national infection peak's magnitude. The columns correspond to the isolated province and the rows to the amount of control effort (0 to 99%).

Control (%)	Groningen	Friesland	Drenthe	Overijssel	Flevoland	Gelderland	Utrecht	Noord-Holland	Zuid-Holland	Zeeland	Noord-Brabant	Limburg
0-40	8,7	8,7	8,7	8,7	8,7	8,7	8,7	8,7	8,7	8,7	8,6	8,7
50	8,7	8,7	8,7	8,7	8,7	8,7	8,7	8,7	8,7	8,7	8,5	8,7
60	8,7	8,7	8,7	8,7	8,7	8,6	8,7	8,6	8,7	8,7	8,4	8,7
70	8,7	8,6	8,7	8,6	8,7	8,6	8,7	8,6	8,6	8,7	8,3	8,7
80	8,6	8,6	8,7	8,6	8,7	8,6	8,7	8,5	8,5	8,7	8,1	8,7
90	8,6	8,6	8,6	8,5	8,7	8,5	8,6	8,2	8,2	8,7	7,8	8,7
99	8,4	8,4	8,5	8,2	8,5	7,8	8,2	7,4	7,5	8,6	7,4	8,3

4.3 Case III: Cut-set travel control

By cut-set control, the Netherlands is divided into two clusters. The people are only allowed to travel within their cluster fully but are restricted to travel to the other. In this case, neighbouring provinces in the Northeast and the Southwest will form the two clusters. Therefore, cluster 1 contains the provinces Groningen, Friesland, Drenthe, Overijssel, Flevoland, and Gelderland. Cluster 2 contains the provinces Utrecht, Noord-holland, Zuid-holland, Zeeland, Noord-Brabant, Limburg.

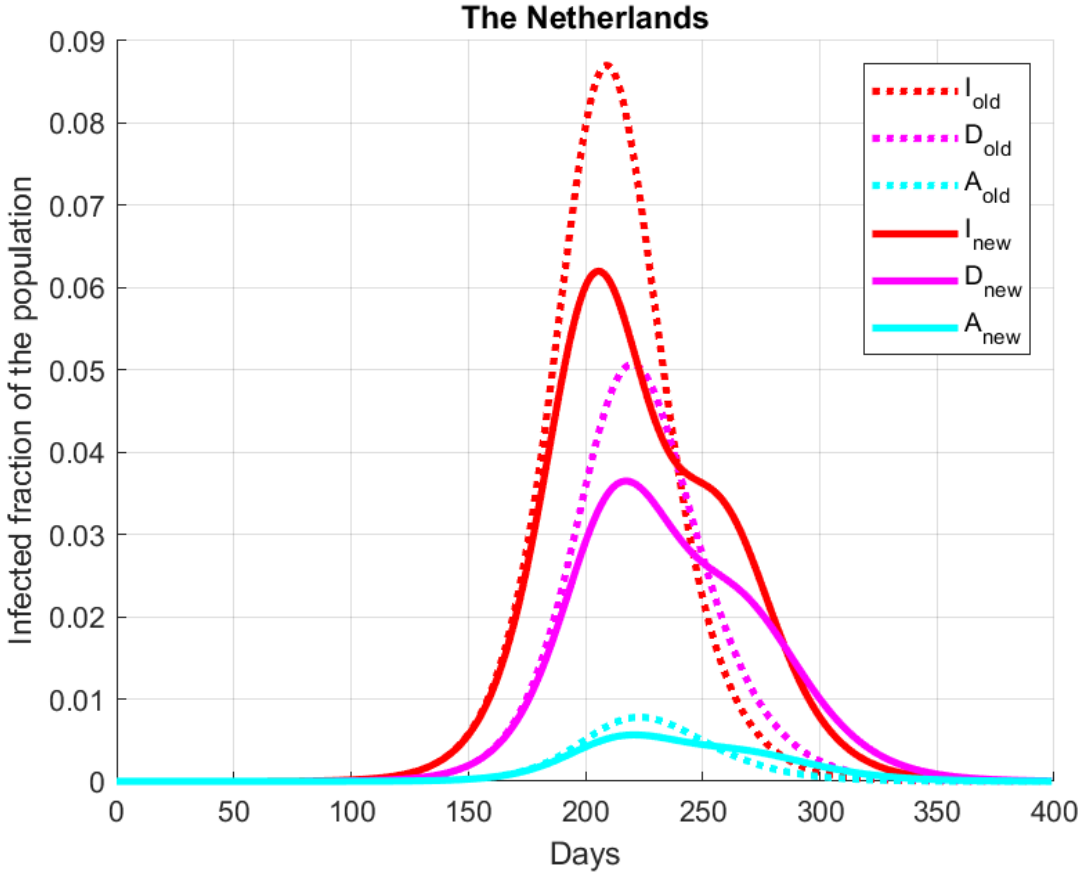

Figure 4.3: The effects of travel restricting measures when the Netherlands is divided into two clusters. The effects on the national infection peak (red), detected peak (magenta), and the amount of deceased(cyan) is shown before (dotted) and after (solid) 99% control is adopted.

Just as with previous travel restricting measures, the total number of cases and deceased will not be affected. However, a change can be found in the timing and magnitude of infections. Figure 4.3 shows the infections (red line), infected detected (magenta line) and acutely symptomatic (cyan line). Here the dotted line represents the original values, and the solid line represents the values when a 99% restriction is applied. It can be seen that the peak of infected will now be flattened and reach a maximum fraction of the population of 6.2%. On the contrary to the previous measures, the peak will be a little bit earlier. The regional plot is shown in figure 4.4. As expected, a delay in the infection peak can be observed in the provinces belonging to the Northeast cluster.

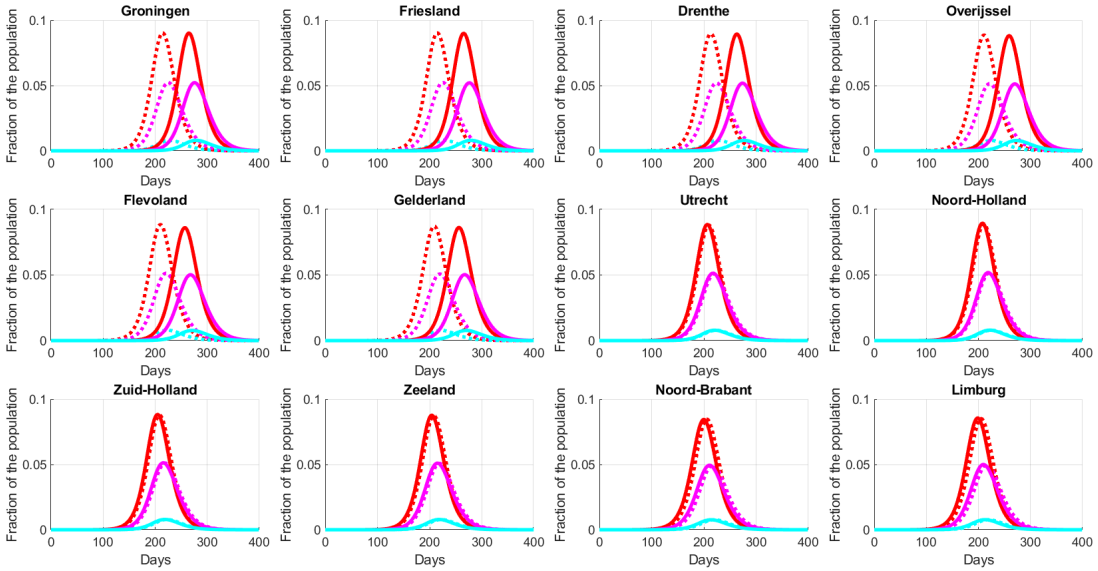

Figure 4.4: The regional effects of travel restricting measures when the Netherlands is divided into two clusters. The effects on the national infections (red), infected detected (magenta), and acutely symptomatic (cyan) is shown before (dotted) and after 99% control (solid) is adopted.

4.4 Case IV: Target cluster travel control

In this case, a target cluster control is simulated. By target cluster control is meant that not just the province with the initial infection is closed, but also three other provinces. The other provinces are the ones who has the most travel from and to Noord-Brabant. So the two clusters are 1) Noord-Braband, Gelderland, Utrecht, Zuid-Holland and 2) Friesland, Groningen Drenthe Overijsel, Flevoland, Noord-Holland, Zeeland, Limburg. As can be seen in figure 4.1, the provinces Limburg and Zeeland are isolated. In this hypothetical case they are allowed to travel through the red provinces to other blue provinces, but only interact in the other blue provinces.

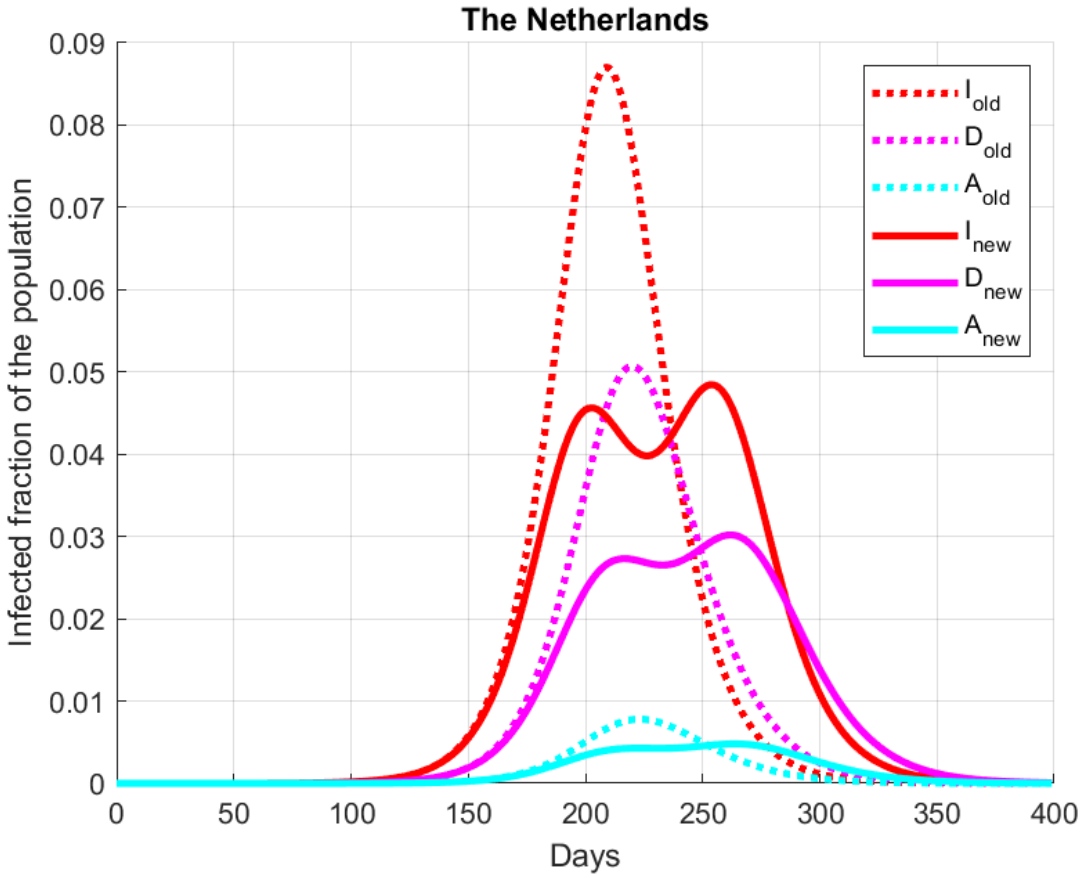

Figure 4.5: The effects of travel restricting measures on the national infections after target cluster control. The effects on the national infections (red), infected detected (magenta), and acutely symptomatic (cyan) is shown before (dotted) and after (solid) 99% control is adopted.

After running the simulation, similar outcomes with target cluster control are found (section 4.3). The total amount of cases and deceased are the same, and a decrease in the national peak can be observed. The national infection peak is now decreased to 5.2% of the population. Interestingly, is this lower than the cut-set control case, while fewer provinces have travel restrictions. Also, the average regional infection peak delay is bigger than with cut-set control (figure D.3 in appendix D). Therefore, it can be concluded that target cluster control is more efficient then cut-set control.

4.5 Robustness travel restriction measures

The literature often gives different estimations of the initial reproduction number R_0 (Billah et al., 2020). Also, the reproduction number changes when NPIs are enforced. Therefore, in this section, the robustness of each travel restrictions are tested by a parameter variation on the β. The β values that are simulated are: 0.14 , 0.17, 0.2, 0.23, 0.26, where 0.14 corresponds to a low R_0 and 0.26 to a high R_0.

4.5.1 Robustness of nationwide and regional travel control

It is found that travel restricting measures change in terms of their effect on the infection peak's timing and magnitude. These effects are plotted in figure 4.6 and section 4.5.1.The left diagram shows the total amount of days the infection peak will be delayed. The right diagram presents the infection peak magnitude decrease. Here the decrease is measured in a percentage of the original peak. From section 4.2 it became clear that regional control only makes sense if it's on

the region with the initial infection. Therefore, the parameter variation for this case is only run for the province Noord-Braband.

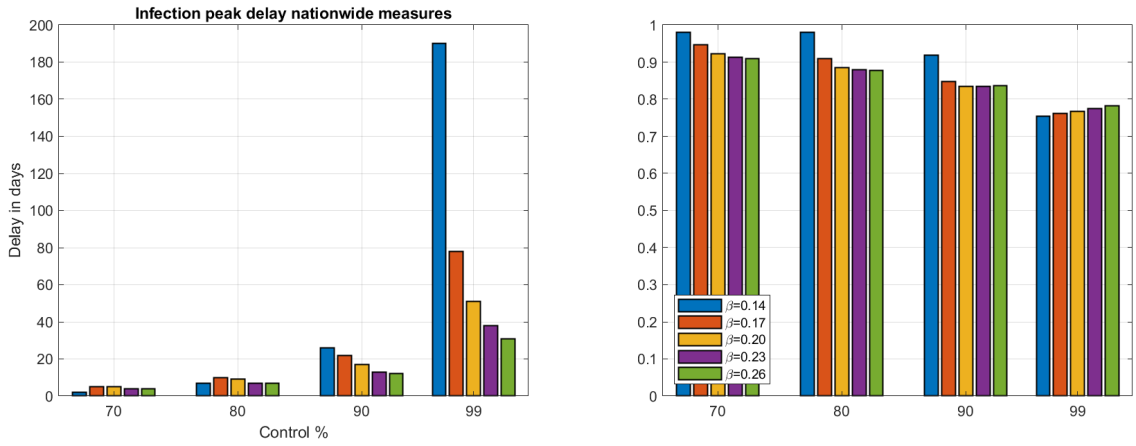

Figure 4.6: The left diagram shows the infection peak delay when nationwide control is applied for different β values. The bars represent the absolute values corresponding to the left y-axis, and the cyan lines represent the percentages corresponding to the right y-axis.The right diagram shows the infection peak magnitude when nationwide control is applied for different β values. Here the decrease in magnitude is given in percentage of the peak when no control effort is applied

The following observations can be made: In combination with a high control effort, lower β values show a significant delay in the absolute infection peak. It can be seen that in both cases, a higher control effort results in a higher peak delay. Furthermore, the infection peak magnitude will decrease almost equally. It can be concluded that both nationwide and regional travel restrictions are more effective when the disease's infectiousness is lower. Therefore, it is more effective in enforcing travel restricting measures simultaneously with other NPIs. For all β values, nationwide control has slightly more impact. Therefore, we conclude that no matter how infectious a disease is, regional control will be more effective than nationwide control.

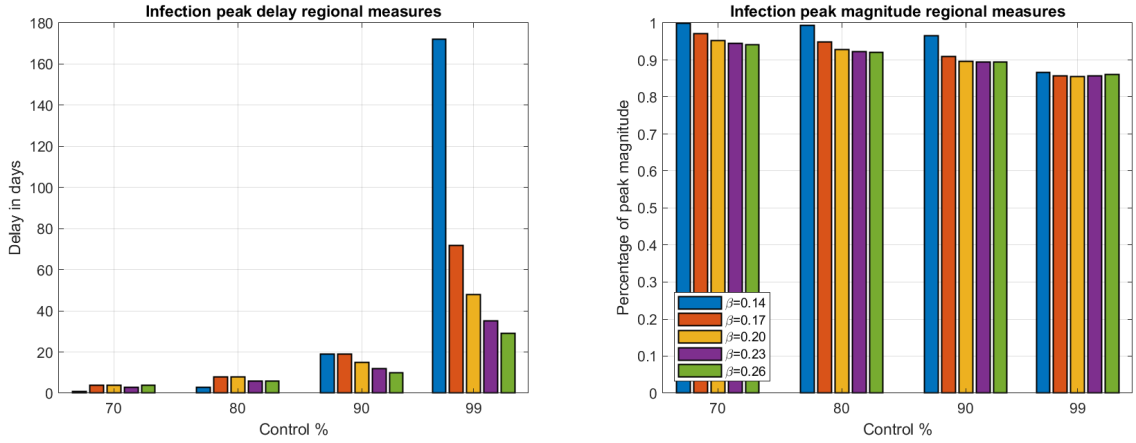

Figure 4.7: The left diagram shows the infection peak delay when regional control is applied for different β values. The bars represent the absolute values corresponding to the left y-axis, and the cyan lines represent the percentages corresponding to the right y-axis. The right diagram shows the infection peak magnitude when nationwide control is applied for different β values. Here, the decrease in magnitude is given in percentage of the peak when no control effort is applied.

4.5.2 Robustness of cut-set and target cluster control

In section 4.3 and section 4.4, a flattening behaviour was observed in the national infection peak, but no significant peak delay. However, the regional peaks in the cluster where no initial infections occurred show a delay. Therefore, it is chosen to compare the change in the national infection peak's magnitude and the regional peaks' delay. The results of this comparison can be found in table 4.3 and table 4.4. For simplicity, the average of the regional peak delay is shown. Here, the difference in the peak magnitude gets higher when the β values rise. Again, lower β values have a higher absolute delay on the regional peaks. So it can be concluded that decreasing the disease's transmission simultaneously increases the travel restrictions' impact. Moreover, the delay in the regional peaks for both cut-set and target cluster control are very similar. However, it can be seen that target cluster control has more impact on the national peak magnitude. Therefore, target cluster control can be considered more effective.

Table 4.3: This table shows the results of the parameter variation on β when 99% of the travel is restricted between the Northeast and the Southwest of the Netherlands. The two most significant changing parameters are compared: the change in magnitude of the national infection peak and the delay of the regional infection peaks.

Parameter variation					
	$\beta = 0,14$	$\beta = 0,17$	$\beta = 0,2$	$\beta = 0,23$	$\beta = 0,26$
Peak magnitude before control	0,49	3,94	8,7	13,5	18,2
Peak magnitude after control	0,37	2,84	6,2	9,64	12,8
Peak magnitude difference	0,12	1,10	2,50	3,86	5,40
Average regional peak time before control	897	335	215	161	130
Average regional peak time after control	1089	413	266	199	161
Average regional peak delay	192	78	51	38	31

Table 4.4: This table shows the results of the parameter variation on β when 99% of the travel is restricted between the target cluster and the rest of the Netherlands. The two most significant changing parameters are compared: the change in magnitude of the national infection peak and the delay of the regional infection peak.

Parameter variation					
	$\beta = 0,14$	$\beta = 0,17$	$\beta = 0,2$	$\beta = 0,23$	$\beta = 0,26$
Peak magnitude before control	0,487	3,96	8,7	13,5	18,2
Peak magnitude after control	0,311	2,22	4,7	7,61	10,3
Peak magnitude difference	0,176	1,74	4	5,89	7,9
Average regional peak time before control	897	335	215	161	130
Average regional peak time after control	1075	411	265	198	160
Average regional peak delay	178	76	50	37	30

Chapter 5: Combining vaccination with travel restricting measures

In this chapter, the possibility of using the infection peak delay and flattening behaviour for fighting COVID-19 is studied. In particular, the travel restriction measures will be simulated together with a vaccination rate. First, the model is adjusted so that it can capture the vaccination dynamics. Then the four cases described in chapter 4 will be repeated but now together with a vaccination rate.

5.1 Model adjustment

Modelling vaccinations can be done in different ways. Cai et al. (2018) models vaccination by adding an extra vaccination compartment to the model. Making an extra compartment provides the possibility to give other properties to that state. Gaff and Schaefer (2009) chooses a more straightforward approach. They added a percentage of the susceptible to the recovered compartment. In this report, the latter option is chosen. This is motivated by the fact that the recovered and vaccinated are assumed to have the same properties, such as staying immune to COVID-19. The new dynamics are shown in equation (5.1),where $\psi \in \mathbb{R}$ denotes the vaccination rate. Note that in this case, it is assumed that only susceptible are vaccinated.

$$\dot{S}_i = -\psi - \sum_{j=1}^{M}\sum_{k=1}^{M} \beta\phi_{ij} S_i - \frac{\phi_{kj} I_k}{N_j} \tag{5.1a}$$

$$\dot{I}_i = \sum_{j=1}^{M}\sum_{k=1}^{M} \beta\phi_{ij} S_i \frac{\phi_{kj} I_k}{N_j} - \gamma_2 I - \xi_2 I - \nu I \tag{5.1b}$$

$$\dot{D}_i = \nu i - \gamma_3 D - \xi_1 D \tag{5.1c}$$

$$\dot{A}_i = \xi_2 I + \xi_1 D - \gamma_1 A - \bar{\mu}(A) \tag{5.1d}$$

$$\dot{R}_i = \gamma_2 I + \gamma_3 D + \gamma_1 A + \psi \tag{5.1e}$$

$$\dot{E}_i = \bar{\mu}(A) \tag{5.1f}$$

5.2 Vaccination rate identification

In this case, the same initial conditions are used as mentioned in chapter 4. It is chosen to use the realistic $\beta = 0.17$. Remember that a $\beta = 0.17$ included social distancing measures, but the infections will still grow sub-exponentially. Furthermore, the vaccination will start after 316 days. This is the time between the first detected case and the first vaccination in the Netherlands (RIVM, 2020) (Rijksoverheid, 2021a).

The vaccination rate highly depends on the approval, operation, delivery and distribution of the vaccines. This makes estimating the actual vaccination rate is difficult. The Netherlands started vaccinating with only 5000 a day, while their goal is to vaccinate more than 70% of the populations within nine months (Rijksoverheid, 2021c). The latter means that around 45.000 people a day need to be vaccinated. Therefore, in this case, three different rates are used: low, medium, and high, corresponding to 5000, 25.000 and 45.000 vaccinations a day. For simplicity, the rates are assumed to be constant,

5.3 Vaccination distribution strategy

There are multiple ways to distribute vaccinations over the provinces. Therefore, three vaccination strategies are studied, and the optimal will be used. The three vaccination strategies are:

1. **Distribute based on population size**. In this strategy, the percentage of the inhabitants in every province is equal to the percentage of vaccinations received. For example, 7,6 % of the population lives in Utrecht, which means that they get 7,6 % of the vaccinations each day.

2. **Distribute by prioritizing one province**. This strategy studies the possibility to vaccinate more in one province than in the others. It is chosen to give the double amount of vaccinations to the prioritized province than to the others. This experiment is repeated twelve times such that every province is prioritized.

3. **Distribute uniformly**. This strategy equally divides the vaccinations over the provinces.

The three strategies are evaluated on the total amount of fatalities. The fatalities are calculated when 25000 vaccines are available per day. The resulting fatalities per strategy are shown in figure figure 5.1.

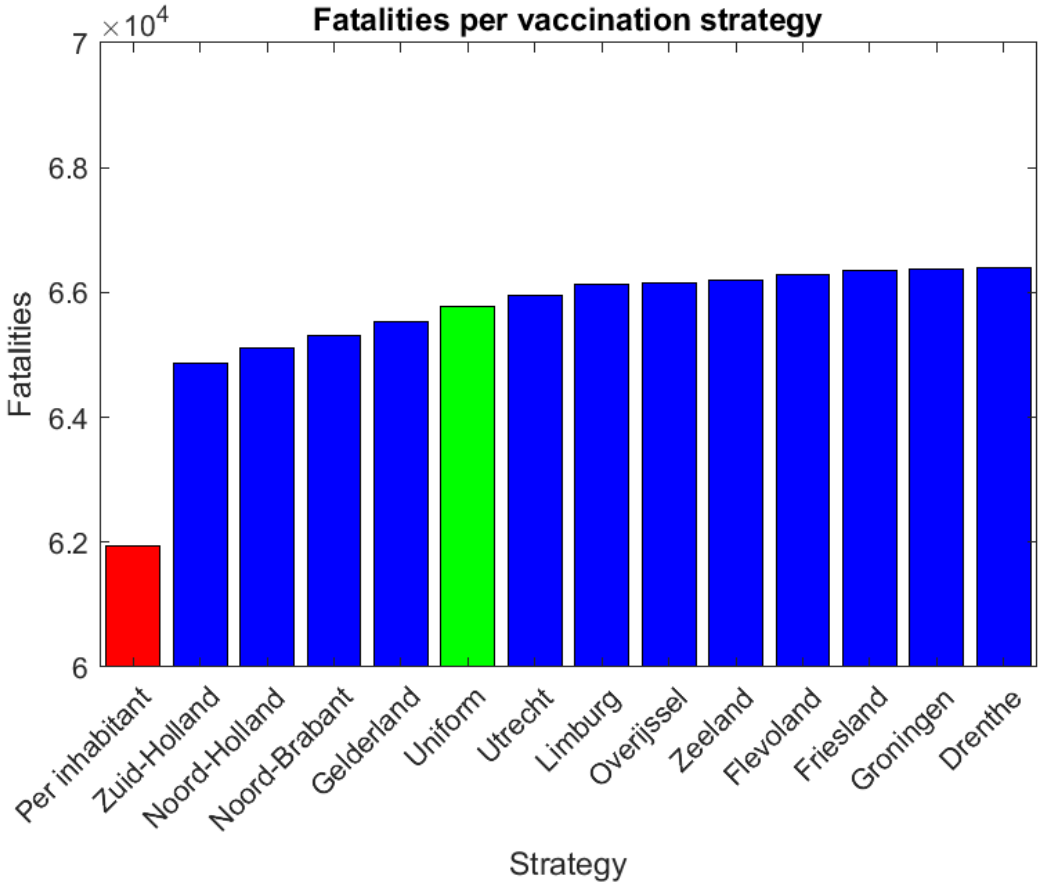

Figure 5.1: This figure compare the number of fatalities when distributing 25000 vaccinations in different ways. The red bar corresponds to strategy 1, 'Distribute based on population size', the green bar to strategy 3 'Distribute uniformly', and the blue bars to strategy 2 'Distribute by prioritizing one province'.

It can be seen that the most optimal strategy is strategy 1: 'Distribute based on population size', which leads to 61800 fatalities. Moreover, If it is chosen to prioritize one province, Zuid-Holland will be the best choice.

5.4 Simulating case I-IV in combination with vaccination

In this section, the effects of travel restricting measures in combination with vaccination strategy one are studied. In figure 5.2 a medium vaccination rate together with regional travel restriction in Noord-Braband is simulated. Here, the dotted line represents the case with no control effort and the solid lines with 99% control effort. It can be seen that the national infection peak greatly decreases. More interestingly, the number of fatalities is significantly reduced.

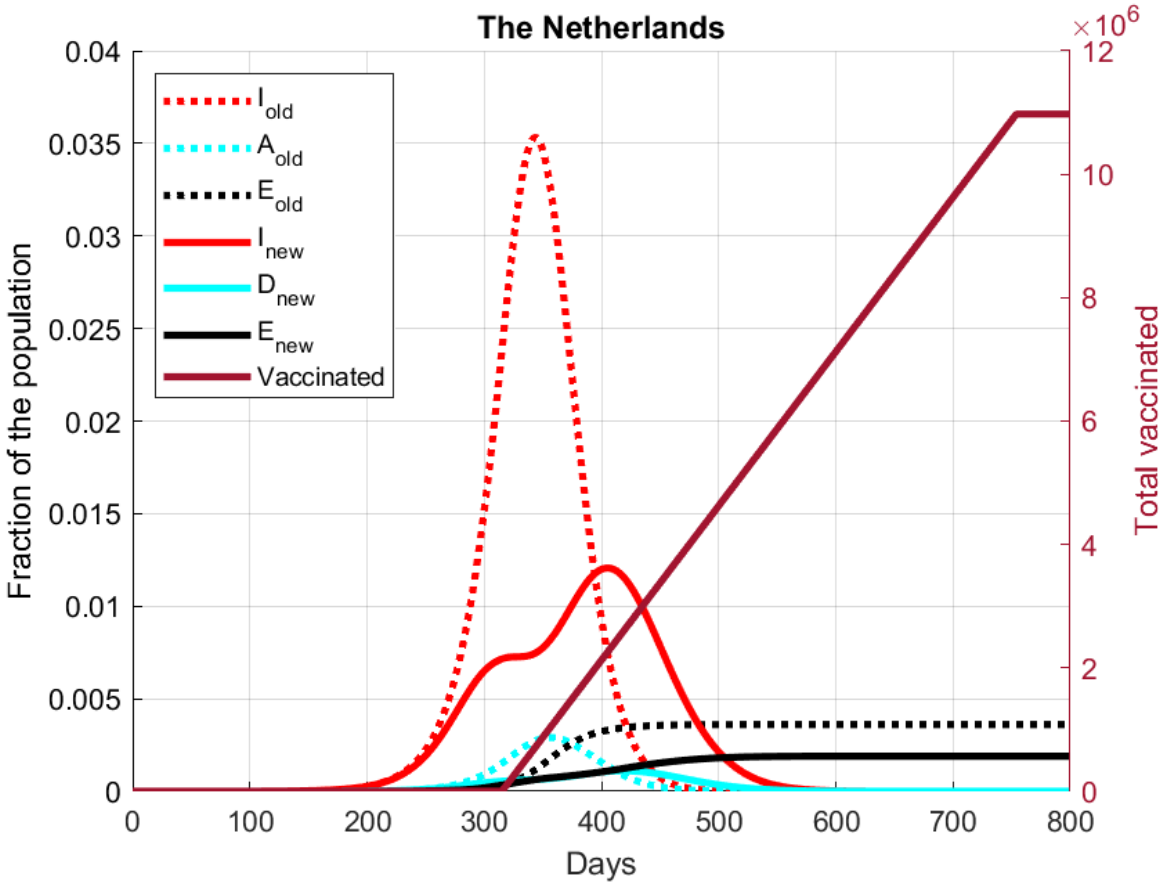

Figure 5.2: Figure showing the effects of regional travel in combination with a medium vaccination rate. The effects on the national infections (red), acutely symptomatic (cyan) and the amount of deceased (black) is shown. The dotted line corresponds to no control effort and the solid to when 99% control effort is applied. The brown line represents the total amount of vaccinated and corresponds to the right y-axis

From figure 5.2 it became clear that vaccinations combined with travel restricting measures lead to fewer fatalities than just by vaccinating. Therefore, cases I-IV are repeated in combination with a vaccination rate, and the number of fatalities is compared. The fatalities by only vaccinating are for a low vaccination rate 76.499, medium vaccination rate, 61.940 and high vaccination rate 52.275. The number of lives saved when travel restrictions are used is shown in figure 5.3 and section 5.4. These lines represent the difference in the amount of deceased between the case where vaccination is applied with the case where vaccination is applied in combination with

travel restrictions. Therefore, these lines can be regarded as lives saved by travel restrictions.

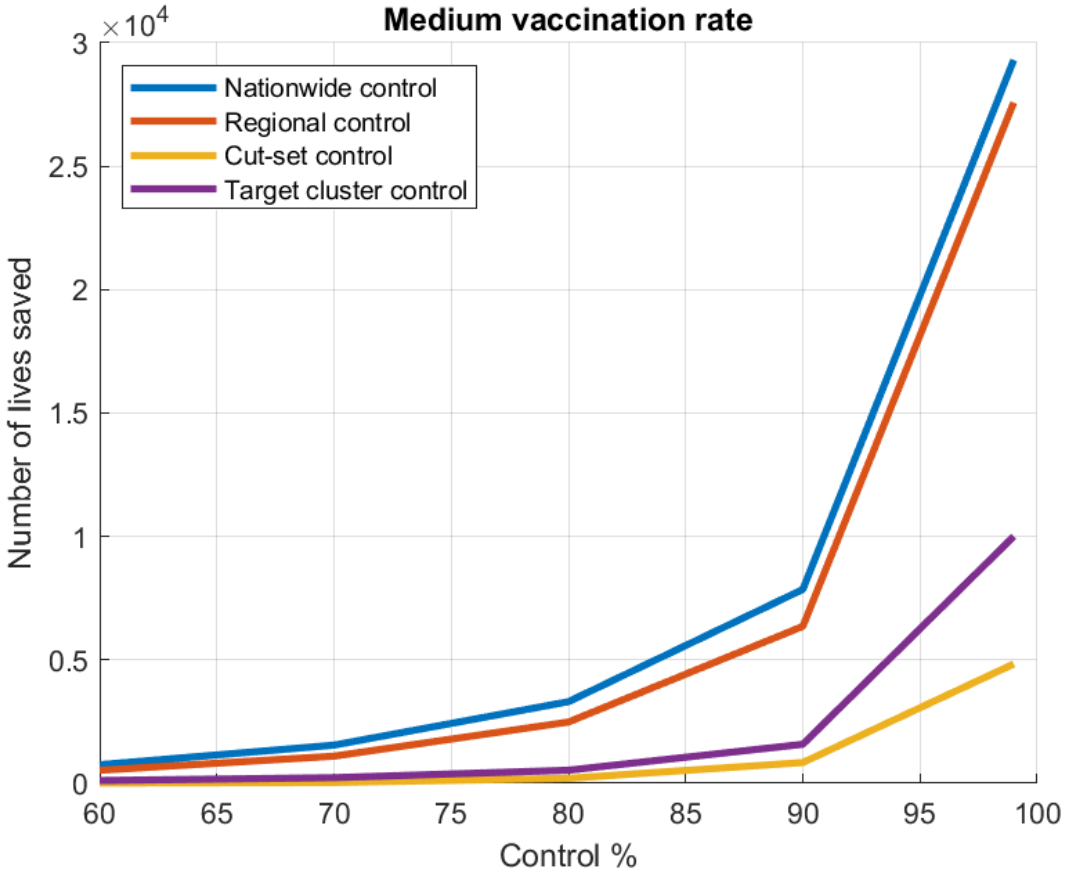

Figure 5.3: Figure showing the number of lives saved by travel restrictions combined with a medium vaccination rate.

Figure 5.3 shows the results of simulations with a medium vaccination rate. It can be seen that the regional control results are again very close to the nationwide control results. Considering the vast impact nationwide control has on the daily, regional control can be regarded as more effective. Moreover, it can be seen that Cut-set control and Target cluster control also lead to saved lives. Therefore, even if there is no delay in the infection peak, still a significant number of lives can be saved. Furthermore, it can be seen that target cluster control saves more lives than separating the Northeast and the Southwest. However, both measures have less impact than regional or nationwide control. It can be concluded that regional control is the most effective travel restricting measure in fighting COVID-19. The same conclusion can be drawn from a low and high vaccination rate (figure 5.4)

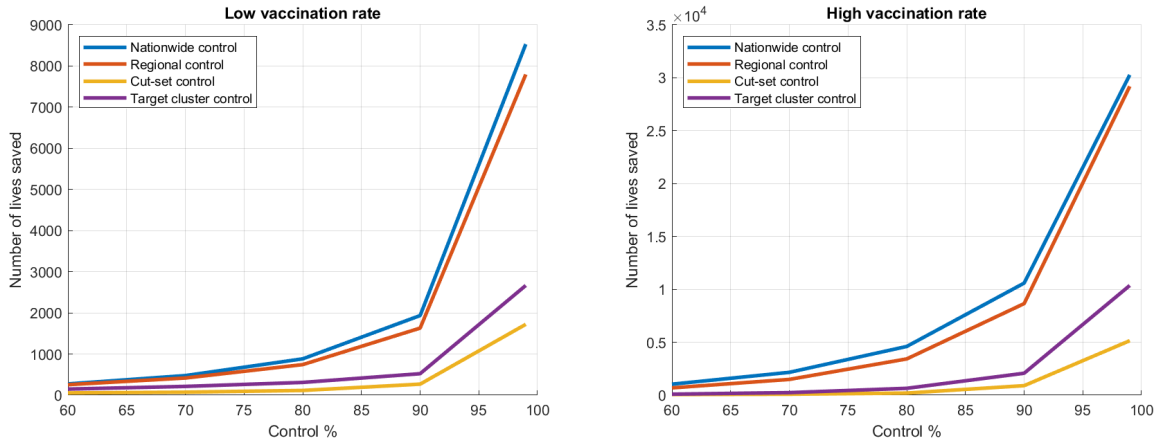

Figure 5.4: Figure showing the number of lives saved by travel restricting measures combined with a low (left) and high (right) vaccination rate.

Chapter 6: Conclusion

In this report, an answer is given to the research question: 'What is the effect of travel restricting measures in the Netherlands on the spreading of the COVID-19 pandemic?' In order to answer this question, a literature study is carried out on spreading disease models. The information out of this literature study is used to construct the metapopulation SIDARE model. After that, the metapopulation SIDARE model is used to simulate different travel restricting measures. The following conclusions can be drawn:

- Despite the assumptions made in the metapopulation SIDARE model, it can be used to accurately predict the amount of infections.
- The effectiveness of travel restricting measure depends on the time of enforcing. When the travel restricting measure are taken immediately, directly after detecting the first infection, a significant delay in the nationwide infection peak can be achieved. By contrast, if the disease has already spread through the whole country, the national infection peak will barely be affected. However, lately imposing travel restriction can affect the regional peaks. A province can delay its local infection peak if it imposes a travel restriction between a region with more infections.
- Regional control is more effective than nationwide control. This statement is supported by the fact that nationwide control causes a delay of 51 versus local control causes a delay of 48 days at 99%. The difference of three days is nearly negligible, given that now only one province has to enforce travel restrictions.
- Splitting the Netherlands into the Northeast and the Southwest only affects the magnitude of the national peak, but not the delay. A bigger effect can be achieved by target cluster control. The target cluster should consist of the neighbouring provinces that have the most travel between them.
- The parameter variation study showed that all forms of travel restricting measures are more effective when the disease's infectiousness is lower. Therefore, it is more effective in enforcing travel restricting measures simultaneously with other NPIs.
- A significant decrease in the amount of deceased by COVID-19 can be achieved when travel restricting measures are combined with a vaccination strategy. The delay in infections enhances the effect of a vaccination strategy. Moreover, regional control results in a slightly lower amount of deceased than nationwide control. The difference is so small that regional control can seen as more effective.

Chapter 7: Discussion

The effects of travel restriction measures found in this report are consistent with the existing literature. Chinazzi et al. (2020) found that the travel ban in China was too late. The reason for this is that the spread has already through the country. However, limiting travel to other countries (where COVID-19 wasn't reported yet) delayed the outbreak in that country. Linka et al. (2020) found similar results for Europe. They mentioned that the overall travel restricting measures were taken a week after the first COVID-19 case in that country.

In this report, travel restricting measures are evaluated on their effectiveness in fighting the pandemic. However, there are some limitations that aren't included in this report. In this report, it is assumed that travel can immediately be reduced by 99%. In reality, the feasibility of this measure is questionable. There will always be people that aren't willing to obey this measure. More importantly, these measures will have a great social and economical impact.

Knowing that travel restricting measures on their own only slow but not halter the spread of a disease begs the question of their desirability. Maier and Brockmann (2020) argues that other NPI's have a lower social impact but can also reach the same effect. In summary, this report only gives insights into travel, restricting measures' effectiveness but is not holistic enough for decision-makers.

Besides the overall usefulness of the results, some technical aspects can be improved. The model can be improved by relaxing some of the assumptions mentioned in section 3.3. The most prominent missing aspect of the metapopulation SIDARE model is the lack of heterogeneity between regions. Heterogeneous infection rates can have an impact on the efficacy of travel restricting measures. However, it is believed that heterogeneity plays a small role in the Netherlands. The reason for this is that the Netherlands is a relatively small country with an almost similar climate, culture and habits in the twelve provinces. Moreover, the regional authorities have little impact on the taken NPIs, resulting in similar rules for every province. Above that, heterogeneous models require significantly more input data, wherein often more assumption will be made. Considering these aspects, a heterogeneous model will not result in major benefits.

An assumption that is believed to have a bigger impact on the results is the last assumption made in section 3.3. This assumption holds that "home stayers" have the same contact rate as travellers, while it's highly likely to be less. Adding this effect to the model will lead to less overall infection. This can be an interesting topic for future research.

This work focuses on the spreading of COVID-19 between the twelve provinces of the Netherlands. By changing the input parameters, this model can be applied to every country in the world. In fact, the model can also be applied on a smaller scale, such as in counties or municipalities.

Chapter 8: Future research

The metapopulation SIDARE model can be used to study a variety of different NPIs. An example that can be thought of is a differentiated feedback lockdown strategy. A differentiated feedback lockdown strategy means that lockdown measures are taken per province based on their infections/ hospitalizations. Della Rossa et al. (2020) studied a differentiated feedback strategy for Italy and found that this can more effective than nationwide lockdown strategies. Here, effective means the amount of control effort required to get a similar effect disease mitigating impact. The metapopulation SIDARE model can be used to repeat this study for the Netherlands.

Future research can be done in improving the metapopulation SIDARE model. The proposed metapopulation SIDARE model estimates travel based on commuting data. However, commuting data is not the only form of travel between regions. Other travel motivations could be shopping, touring, hobbies etc. Estimating travel on the actual amount of moving vehicles can be more accurate. Moreover, travel from and to other countries can be modelled. This opens new research topics such as: what is the impact of the imported cases on the spreading of COVID-19 in the Netherlands? Another improvement can be made in considering more factors that are usefull for decison-makers. The model can be extended to a version that considers the economical impact of the travel restricting measures. After that, the travel restricting measures can be compared to other NPIs.

At the time of writing, the Netherlands has already started vaccinating. The current vaccination strategy prioritises vaccinating the elderly and other risk groups first (Rijksoverheid, 2021c). The idea behind this strategy is that it lowers the pressure on the ICU capacity. However, putting ethical considerations aside, it can be argued that this is not the most effective strategy. Miller and Hyman (2007) suggests that vaccination should focus on those people with the most unvaccinated contacts. The next best strategy is to vaccinate the people that have the most contacts. This theory can be used in combination with the metapopulation SIDARE model to test optimal vaccination strategies.

Finally, it is important to notice that the metapopulation SIDARE model's subpopulations don't necessarily have to represented regions. The subpopulation can also represent the elderly, risk groups or something else. In this way, whole different studies can be conducted. An example could be the plan of herstel-NL, which wants to split the population into two groups (https://herstel-nl.nl). One of these groups are able to live a normal life, and the other group (the risk group) will be isolated as much as possible. A challenging part of this study will be how to model the contact rates between those groups.

Bibliography

Aguiar, M., Ortuondo, E. M., Van-Dierdonck, J. B., Mar, J., and Stollenwerk, N. (2020). Modelling covid 19 in the basque country from introduction to control measure response. Scientific Reports, 10(1):1–16.

Ahn, H. J. and Hassibi, B. (2013). Global dynamics of epidemic spread over complex networks. In 52nd IEEE Conference on Decision and Control, pages 4579–4585. IEEE.

Andreas Kasis, Stelios Timotheou, N. M.-M. P. (2021). Optimal government intervention strategies to mitigate the covid-19 pandemic effects. This research has not been published yet.

Arino, J. and Van den Driessche, P. (2003). A multi-city epidemic model. Mathematical Population Studies, 10(3):175–193.

Billah, M. A., Miah, M. M., and Khan, M. N. (2020). Reproductive number of coronavirus: A systematic review and meta-analysis based on global level evidence. PloS one, 15(11):e0242128.

Birge, J. R., Candogan, O., and Feng, Y. (2020). Controlling epidemic spread: Reducing economic losses with targeted closures. University of Chicago, Becker Friedman Institute for Economics Working Paper, (2020-57).

Cai, L.-M., Li, Z., and Song, X. (2018). Global analysis of an epidemic model with vaccination. Journal of Applied Mathematics and Computing, 57(1):605–628.

CBS (2018). Verkeersintensiteit; rijkswegen. `https://opendata.cbs.nl/statline/#/CBS/nl/dataset/82855NED/table,Accessed:02-11-2020`.

Chinazzi, M., Davis, J. T., Ajelli, M., Gioannini, C., Litvinova, M., Merler, S., y Piontti, A. P., Mu, K., Rossi, L., Sun, K., et al. (2020). The effect of travel restrictions on the spread of the 2019 novel coronavirus (covid-19) outbreak. Science, 368(6489):395–400.

Della Rossa, F., Salzano, D., Di Meglio, A., De Lellis, F., Coraggio, M., Calabrese, C., Guarino, A., Cardona-Rivera, R., De Lellis, P., Liuzza, D., et al. (2020). A network model of italy shows that intermittent regional strategies can alleviate the covid-19 epidemic. Nature Communications, 11(1):1–9.

Djidjou Demasse, R., Michalakis, Y., Choisy, M., Sofonea, M., and Alizon, S. (2020). Optimal covid-19 epidemic control until vaccine deployment.

Dorogovtsev, S. (2010). Complex networks. Oxford: Oxford University Press.

Duan, W., Fan, Z., Zhang, P., Guo, G., and Qiu, X. (2015). Mathematical and computational approaches to epidemic modeling: a comprehensive review. Frontiers of Computer Science, 9(5):806–826.

Gaff, H. and Schaefer, E. (2009). Optimal control applied to vaccination and treatment strategies for various epidemiological models. Mathematical Biosciences & Engineering, 6(3):469.

Ganesh, A., Massoulié, L., and Towsley, D. (2005). The effect of network topology on the spread of epidemics. In Proceedings IEEE 24th Annual Joint Conference of the IEEE Computer and Communications Societies., volume 2, pages 1455–1466. IEEE.

Gatto, M., Bertuzzo, E., Mari, L., Miccoli, S., Carraro, L., Casagrandi, R., and Rinaldo, A. (2020). Spread and dynamics of the covid-19 epidemic in italy: Effects of emergency containment measures. Proceedings of the National Academy of Sciences, 117(19):10484–10491.

Giordano, G., Blanchini, F., Bruno, R., Colaneri, P., Filippo, A., Matteo, A., and Colaneri, M. (2020). Modelling the covid-19 epidemic and implementation of population-wide interventions in italy. Nature Medicine, 26:1–6.

Gross, T., D'Lima, C. J. D., and Blasius, B. (2006). Epidemic dynamics on an adaptive network. Physical review letters, 96(20):208701.

health agency of sweden, P. (2020). The infection fatality rate of covid-19 in stockholm. Accessed: 29-1-2020.

Hethcote, H. W. (1978). An immunization model for a heterogeneous population. Theoretical population biology, 14(3):338–349.

Hethcote, H. W. and Van den Driessche, P. (1991). Some epidemiological models with nonlinear incidence. Journal of Mathematical Biology, 29(3):271–287.

Johnson, K. E., Song, T., Greenbaum, B., and Ghedin, E. (2017). Getting the flu: 5 key facts about influenza virus evolution. PLoS pathogens, 13(8):e1006450.

Kephart, J. O. and White, S. R. (1992). Directed-graph epidemiological models of computer viruses. In Computation: the micro and the macro view, pages 71–102. World Scientific.

Kermack, W. O. and McKendrick, A. G. (1927). A contribution to the mathematical theory of epidemics. Proceedings of the royal society of london. Series A, Containing papers of a mathematical and physical character, 115(772):700–721.

Lajmanovich, A. and Yorke, J. A. (1976). A deterministic model for gonorrhea in a nonhomogeneous population. Mathematical Biosciences, 28(3-4):221–236.

Li, M. Y., Graef, J. R., Wang, L., and Karsai, J. (1999). Global dynamics of a seir model with varying total population size. Mathematical biosciences, 160(2):191–213.

Li, M. Y. and Muldowney, J. S. (1995). Global stability for the seir model in epidemiology. Mathematical biosciences, 125(2):155–164.

Linka, K., Peirlinck, M., Sahli Costabal, F., and Kuhl, E. (2020). Outbreak dynamics of covid-19 in europe and the effect of travel restrictions. Computer Methods in Biomechanics and Biomedical Engineering, 23(11):710–717.

Maier, B. F. and Brockmann, D. (2020). Effective containment explains subexponential growth in recent confirmed covid-19 cases in china. Science, 368(6492):742–746.

Max Roser, Hannah Ritchie, E. O.-O. and Hasell, J. (2020). Coronavirus pandemic (covid-19). Our World in Data. https://ourworldindata.org/coronavirus.

Mei, W., Mohagheghi, S., Zampieri, S., and Bullo, F. (2017). On the dynamics of deterministic epidemic propagation over networks. Annual Reviews in Control, 44:116–128.

Mendoza, C. I. (2020). Inhomogeneous mixing and asynchronic transmission between local outbreaks account for the spread of covid-19 epidemics. medRxiv.

Miller, J. C. and Hyman, J. M. (2007). Effective vaccination strategies for realistic social networks. Physica A: Statistical Mechanics and its Applications, 386(2):780–785. Disorder and Complexity.

Moreno, Y., Pastor-Satorras, R., and Vespignani, A. (2002). Epidemic outbreaks in complex heterogeneous networks. The European Physical Journal B-Condensed Matter and Complex Systems, 26(4):521–529.

Nations, U. (2020). United nations - department of economic and social affairs - population dynamics. Accessed: 27-1-2020.

Nowzari, C., Preciado, V. M., and Pappas, G. J. (2014). Stability analysis of generalized epidemic models over directed networks. In 53rd IEEE Conference on Decision and Control, pages 6197–6202. IEEE.

Nowzari, C., Preciado, V. M., and Pappas, G. J. (2015). Optimal resource allocation for control of networked epidemic models. IEEE Transactions on Control of Network Systems, 4(2):159–169.

Nowzari, C., Preciado, V. M., and Pappas, G. J. (2016). Analysis and control of epidemics: A survey of spreading processes on complex networks. IEEE Control Systems Magazine, 36:26–46.

Pastor-Satorras, R., Castellano, C., Van Mieghem, P., and Vespignani, A. (2015). Epidemic processes in complex networks. Reviews of modern physics, 87(3):925.

Perez-Saez, J., Lauer, S. A., Kaiser, L., Regard, S., Delaporte, E., Guessous, I., Stringhini, S., Azman, A. S., Alioucha, D., Arm-Vernez, I., et al. (2020). Serology-informed estimates of sars-cov-2 infection fatality risk in geneva, switzerland. The Lancet Infectious Diseases.

Pica, N. and Bouvier, N. M. (2012). Environmental factors affecting the transmission of respiratory viruses. Current opinion in virology, 2(1):90–95.

Rhodes, A., Ferdinande, P., Flaatten, H., Guidet, B., Metnitz, P. G., and Moreno, R. P. (2012). The variability of critical care bed numbers in europe. Intensive care medicine, 38(10):1647–1653.

Rijksoverheid (2021a). Eerste vaccinatie op 8 januari 2021. Accessed: 3-2-2020.

Rijksoverheid (2021b). Persconferenties coronavirus. `https://www.rijksoverheid.nl/onderwerpen/coronavirus-covid-19/coronavirus-beeld-en-video/videos-persconferenties`. Accessed on 24-1-2021.

Rijksoverheid (2021c). Vaccinatiestrategie: stroomschema (versie 4 januari 2021). Accessed: 3-2-2020.

RIVM (2020). Patiënt met nieuw coronavirus in nederland. Accessed: 18-1-2020.

Sattenspiel, L., Dietz, K., et al. (1995). A structured epidemic model incorporating geographic mobility among regions. Mathematical biosciences, 128(1):71–92.

Shaw, J. (2007). The sars scare. Harvard Magazine, 109(4):48.

Shen, C., Chen, H., and Hou, Z. (2012). Strategy to suppress epidemic explosion in heterogeneous metapopulation networks. Phys. Rev. E, 86:036114.

Van Aken, J. E. and Berends, H. (2018). Problem solving in organizations. Cambridge university press.

Van Mieghem, P., Omic, J., and Kooij, R. (2008). Virus spread in networks. IEEE/ACM Transactions On Networking, 17(1):1–14.

Verity, R., Okell, L. C., Dorigatti, I., Winskill, P., Whittaker, C., Imai, N., Cuomo-Dannenburg, G., Thompson, H., Walker, P. G., Fu, H., Dighe, A., Griffin, J. T., Baguelin, M., Bhatia, S., Boonyasiri, A., Cori, A., Cucunubá, Z., FitzJohn, R., Gaythorpe, K., Green, W., Hamlet, A., Hinsley, W., Laydon, D., Nedjati-Gilani, G., Riley, S., van Elsland, S., Volz, E., Wang, H.,

Wang, Y., Xi, X., Donnelly, C. A., Ghani, A. C., and Ferguson, N. M. (2020). Estimates of the severity of covid-19 disease. medRxiv.

Wang, Y., Chakrabarti, D., Wang, C., and Faloutsos, C. (2003). Epidemic spreading in real networks: An eigenvalue viewpoint. In 22nd International Symposium on Reliable Distributed Systems, 2003. Proceedings., pages 25–34. IEEE.

Watts, D. J. and Strogatz, S. H. (1998). Collective dynamics of 'small-world'networks. nature, 393(6684):440–442.

WHO (2020a). Coronavirus disease (covid-19). Last accessed 16 September 2017.

WHO (2020b). Coronavirus disease (covid-2019) situation reports. https://www.who.int/docs/default-source/coronaviruse/situation-reports/20201020-weekly-epi-update-10.pdf.

WHO (2020c). Report of the who-china joint mission on coronavirus disease 2019 (covid-19). https://www.who.int/publications/i/item/report-of-the-who-china-joint-mission-on-coronavirus-disease-2019-(covid-19).

Wieringa, R. J. (2014). Design science methodology for information systems and software engineering. Springer.

Xia, C., Wang, L., Sun, S., and Wang, J. (2012). An sir model with infection delay and propagation vector in complex networks. Nonlinear Dynamics, 69(3):927–934.

Appendix A: Differential equations

Differential equations SEAIRD model

$$
\begin{aligned}
&\dot{S} = -\lambda S - \mu\left[I_s\right] S \\
&\dot{E}_m = p\lambda S - \varepsilon E_m - \mu\left[I_s\right] E_m + p\nu \\
&\dot{A}_m = \varepsilon E_m - \sigma A_m - \mu\left[I_s\right] A_m \\
&\dot{I}_m = \sigma A_m - \left(\gamma_m + \mu\left[I_s\right]\right) I_m \\
&\dot{R}_m = \gamma_m I_m - \mu\left[I_s\right] R_m \\
&\dot{E}_s = (1-p)\lambda S - \varepsilon E_s - \mu\left[I_s\right] E_s + (1-p)\nu \\
&\dot{A}_s = \varepsilon E_s - \sigma A_s - \mu\left[I_s\right] A_s \\
&\dot{I}_s = \sigma A_s - \left(\gamma_s + \mu\left[I_s\right] + \alpha\left[I_s\right]\right) I_s \\
&\dot{R}_s = \gamma_s I_s - \mu\left[I_s\right] R_s \\
&\dot{D} = \alpha\left[I_s\right] I_s + \mu\left[I_s\right] N \\
&\text{with} \\
&N = S + E + A + I + R \\
&E = E_s + E_m, \quad A = A_s + A_m, \quad I = I_s + I_m, \quad R = R_s + R_m \\
&\lambda = (1-c)\left(\beta_A\left(A_s + A_m\right) + \beta_I\left(I_m + \xi I_s\right)\right)
\end{aligned}
$$

Differential equations SIDHARTE model

$$
\begin{aligned}
&S(t) = -S(t)(aI(t) + \beta D(t) + rA(t) + \delta R(t)) \\
&I(t) = S(t)(al(t) + \beta D(t) + yA(t) + \delta R(t)) - (e + \zeta + \lambda)I(t) \\
&\dot{D}(t) = eI(t) - (\eta + \rho)D(t) \\
&A(t) = \zeta I(t) - (\theta + \mu + \kappa)A(t) \\
&\dot{k}(t) = \eta D(t) + \theta A(t) - (\nu + \xi)R(t) \\
&\dot{T}(t) = \mu A(t) + \nu R(t) - (d + z)T(t) \\
&H(t) = \lambda I(t) + \rho D(t) + \kappa A(t) + \xi R(t) + \sigma T(t) \\
&E(t) = rT(t)
\end{aligned}
$$

Differential equations SEIIR model

$$
S_i' = \mu N_i - \beta \sum_j \underbrace{S_i \tau_{ij}}_{\text{Time agent } \in S_i \text{ spends at } j} \Bigg(\underbrace{\frac{\sum_k I_k^c \tau_{kj}}{\sum_k N_k \tau_{kj}}}_{\text{Fraction of clinical infected at } j} + \alpha \underbrace{\frac{\sum_k I_k^{sc} \tau_{kj}}{\sum_k N_k \tau_{kj}}}_{\text{subclinical infected at } j} \Bigg) (-\mu S_i
$$

$$
E_i' = \beta \sum_j \underbrace{S_i \tau_{ij}}_{\text{Time agent } \in S_i \text{ spends at } j} \Bigg(\underbrace{\frac{\sum_k I_k^c \tau_{kj}}{\sum_k N_k \tau_{kj}}}_{\text{Fraction of clinical infected at } j} + \alpha \underbrace{\frac{\sum_k I_k^{sc} \tau_{kj}}{\sum_k N_k \tau_{kj}}}_{\text{subclinical infected at } j} \Bigg) - (\mu + \kappa) E_i
$$

$$
\begin{aligned}
&I_i^{c'} = \rho\kappa E_i - (\mu + \gamma) I_i^c \\
&I_i^{sc'} = (1-\rho)\kappa E_i - (\mu + \gamma) I_i^{sc} \\
&R_i' \gamma I_i^c + \gamma I_i^{sc} - \mu R_i
\end{aligned}
$$

Differential equations SIQHDR model

$$
\begin{aligned}
\dot{S}_i &= -\sum_{j=1}^{M}\sum_{k=1}^{M} \rho_j \beta \phi_{ij}(t) S_i \frac{\phi_{kj}(t) I_k}{N_j^p} \\
\dot{I}_i &= \sum_{j=1}^{M}\sum_{k=1}^{M} \rho_j \beta \phi_{ij}(t) S_i \frac{\phi_{kj}(t) I_k}{N_j^p} - \alpha_i I_i - \psi_i I_i - \gamma I_i \\
\dot{Q}_i &= \alpha_i I_i - x_i'' Q_i - \eta_i^Q Q_i + \kappa_i^Q H_i \\
\dot{H}_i &= \kappa_i^M Q_i + \psi_i I_i - \eta_i^M H_i - \kappa_i^Q H_i - \zeta \left(H_i / T_i^H \right) H_i \\
\dot{D}_i &= \zeta \left(H_i / T_i^H \right) H_i \\
\dot{R}_i &= y I_i + \eta_i^Q Q_i + \eta_i^H H_i \\
N_i^p &= \sum_{k=1}^{M} \phi_{bi}(t) \left(S_k + I_k + R_k \right)
\end{aligned}
$$

Differential equations SHARUCD model

$$
\begin{aligned}
\dot{S} &= -\beta \frac{S}{N}(H + \phi A + \varrho N) \\
\dot{H} &= \eta\beta \frac{S}{N}(H + \phi A + \varrho N) - (\gamma + \mu + v) H \\
\dot{A} &= (1-\eta)\beta \frac{S}{N}(H + \phi A + \varrho N) - \gamma A \\
\dot{R} &= \gamma(H + U + A) \\
\dot{U} &= v\eta\beta \frac{S}{N}(H + \phi A + \varrho N) - (\gamma + \mu) U \\
\dot{C_H} &= \eta\beta \frac{S}{N}(H + \phi A + \varrho N) \\
\dot{C_A} &= \xi \cdot (1-\eta)\beta \frac{S}{N}(H + \phi A + \varrho N) \\
\dot{C_R} &= \gamma(H + U + \xi A) \\
\dot{C_U} &= vH \\
\dot{D} &= \mu(H + U)
\end{aligned}
$$

Appendix B: Map of the Netherlands

Figure B.1: A map of the Netherlands with its twelve provinces

Appendix C: Adjacency matrices

$$\text{Adjacency matrix case I } = \begin{bmatrix} 1&0&0&0&0&0&0&0&0&0&0&0\\ 0&1&0&0&0&0&0&0&0&0&0&0\\ 0&0&1&0&0&0&0&0&0&0&0&0\\ 0&0&0&1&0&0&0&0&0&0&0&0\\ 0&0&0&0&1&0&0&0&0&0&0&0\\ 0&0&0&0&0&1&0&0&0&0&0&0\\ 0&0&0&0&0&0&1&0&0&0&0&0\\ 0&0&0&0&0&0&0&1&0&0&0&0\\ 0&0&0&0&0&0&0&0&1&0&0&0\\ 0&0&0&0&0&0&0&0&0&1&0&0\\ 0&0&0&0&0&0&0&0&0&0&1&0\\ 0&0&0&0&0&0&0&0&0&0&0&1 \end{bmatrix} \tag{C.1}$$

$$\text{Adjacency matrix case II } = \begin{bmatrix} 1&1&1&1&1&1&1&1&1&1&0&1\\ 1&1&1&1&1&1&1&1&1&1&0&1\\ 1&1&1&1&1&1&1&1&1&1&0&1\\ 1&1&1&1&1&1&1&1&1&1&0&1\\ 1&1&1&1&1&1&1&1&1&1&0&1\\ 1&1&1&1&1&1&1&1&1&1&0&1\\ 1&1&1&1&1&1&1&1&1&1&0&1\\ 1&1&1&1&1&1&1&1&1&1&0&1\\ 1&1&1&1&1&1&1&1&1&1&0&1\\ 1&1&1&1&1&1&1&1&1&1&0&1\\ 0&0&0&0&0&0&0&0&0&0&1&0\\ 1&1&1&1&1&1&1&1&1&1&0&1 \end{bmatrix} \tag{C.2}$$

Note that equation (C.2) is for the particular case where Noord-Braband is isolated. If another provinces is selected, the zero row and column shifts.

$$\text{Adjacency matrix case III } = \begin{bmatrix} 1&1&1&1&1&1&0&0&0&0&0&0\\ 1&1&1&1&1&1&0&0&0&0&0&0\\ 1&1&1&1&1&1&0&0&0&0&0&0\\ 1&1&1&1&1&1&0&0&0&0&0&0\\ 1&1&1&1&1&1&0&0&0&0&0&0\\ 1&1&1&1&1&1&0&0&0&0&0&0\\ 0&0&0&0&0&0&1&1&1&1&1&1\\ 0&0&0&0&0&0&1&1&1&1&1&1\\ 0&0&0&0&0&0&1&1&1&1&1&1\\ 0&0&0&0&0&0&1&1&1&1&1&1\\ 0&0&0&0&0&0&1&1&1&1&1&1\\ 0&0&0&0&0&0&1&1&1&1&1&1 \end{bmatrix} \tag{C.3}$$

$$\text{Adjacency matrix case IV} = \begin{bmatrix} 1 & 1 & 1 & 1 & 1 & 0 & 0 & 1 & 0 & 1 & 0 & 1 \\ 1 & 1 & 1 & 1 & 1 & 0 & 0 & 1 & 0 & 1 & 0 & 1 \\ 1 & 1 & 1 & 1 & 1 & 0 & 0 & 1 & 0 & 1 & 0 & 1 \\ 1 & 1 & 1 & 1 & 1 & 0 & 0 & 1 & 0 & 1 & 0 & 1 \\ 1 & 1 & 1 & 1 & 1 & 0 & 0 & 1 & 0 & 1 & 0 & 1 \\ 0 & 0 & 0 & 0 & 0 & 1 & 1 & 0 & 1 & 0 & 1 & 0 \\ 0 & 0 & 0 & 0 & 0 & 1 & 1 & 0 & 1 & 0 & 1 & 0 \\ 1 & 1 & 1 & 1 & 1 & 0 & 0 & 1 & 0 & 1 & 0 & 1 \\ 0 & 0 & 0 & 0 & 0 & 1 & 1 & 0 & 1 & 0 & 1 & 0 \\ 1 & 1 & 1 & 1 & 1 & 0 & 0 & 1 & 0 & 1 & 0 & 1 \\ 0 & 0 & 0 & 0 & 0 & 1 & 1 & 0 & 1 & 0 & 1 & 0 \\ 1 & 1 & 1 & 1 & 1 & 0 & 0 & 1 & 0 & 1 & 0 & 1 \end{bmatrix} \tag{C.4}$$

Appendix D: Plots

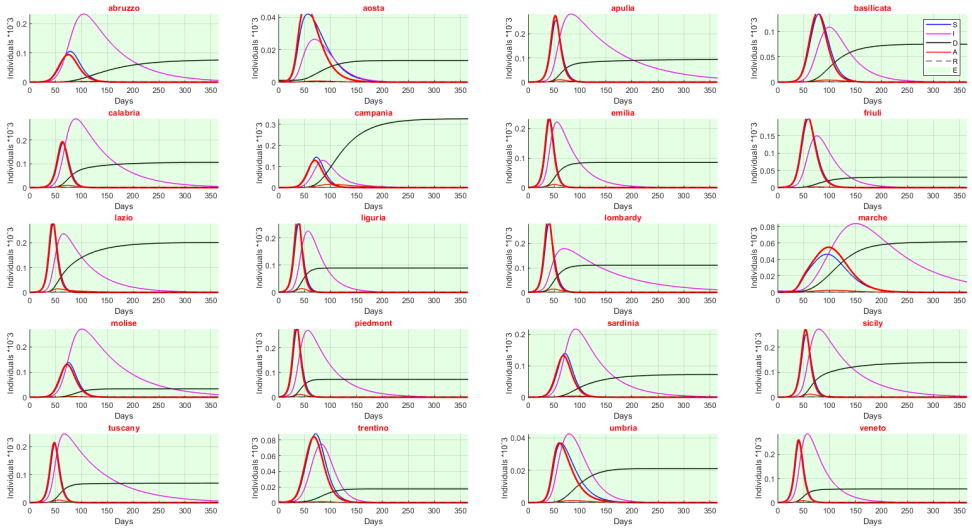

Figure D.1: These graphs show the simulated number of infections by the metapopulation SIDARE model (red) compared with the SIDQHR model (blue) by Della Rossa et al. (2020)

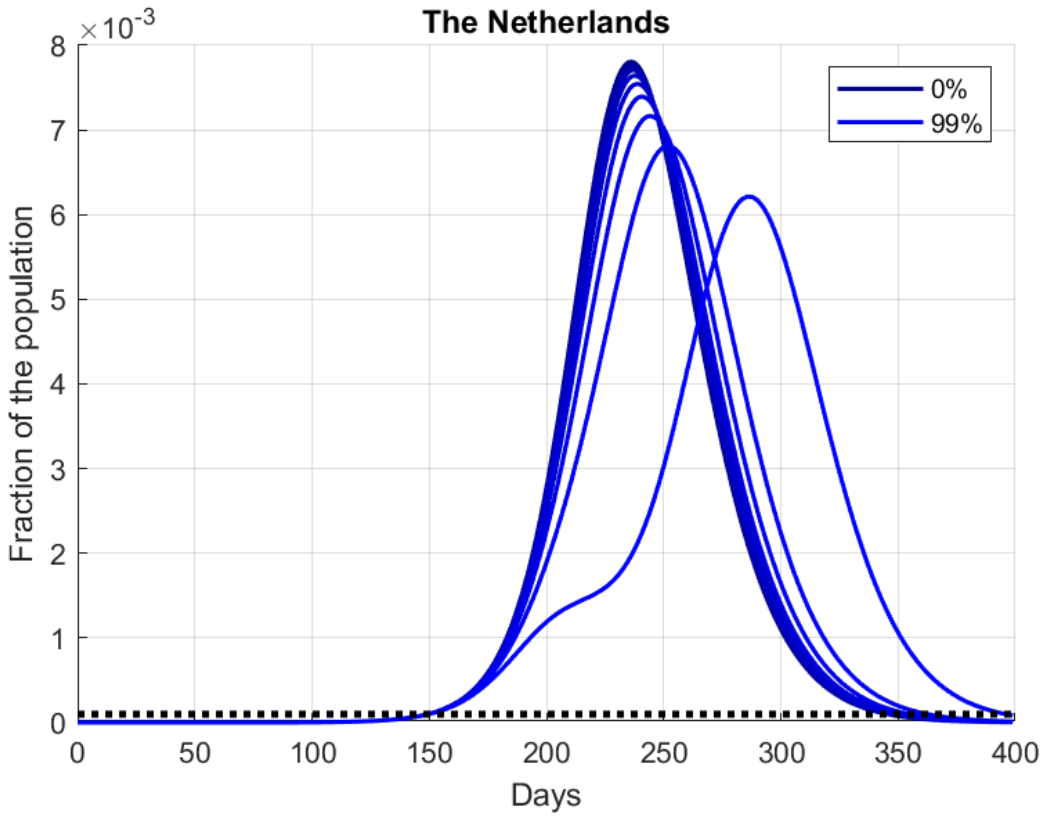

Figure D.2: The effect of nationwide travel restrictions from 0 to 99% on the national Acutely Symptomatic peak. The lightest colour shows the highest control effort. The black dotted line represents the ICU capacity of the Netherlands

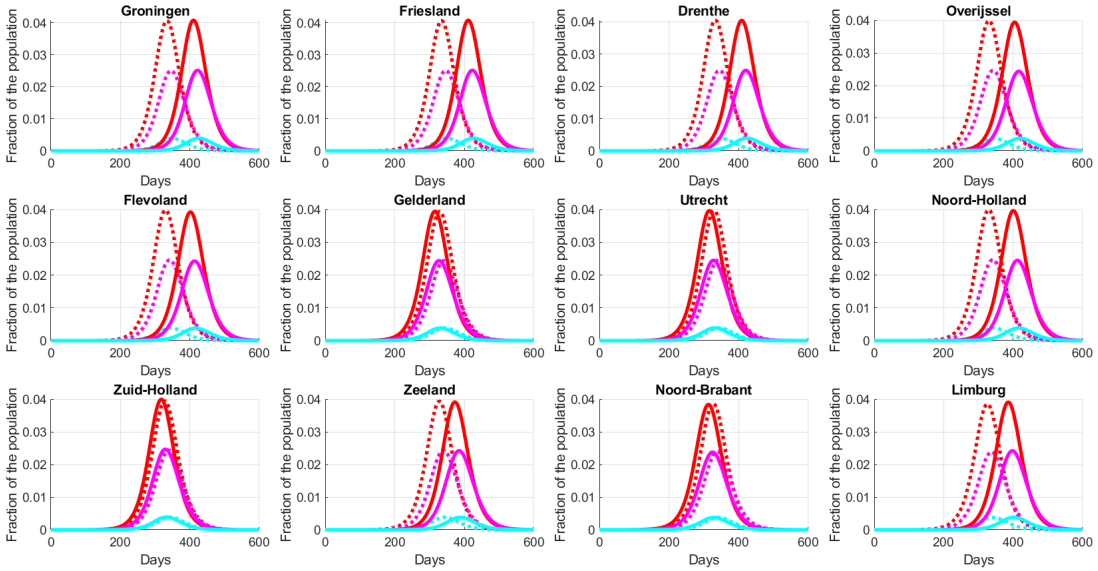

Figure D.3: Regional plot showing the effects of restricting the travel between the the target cluster and the rest of the Netherlands 99%

Appendix E: Matlab code

Listing E.1: SIDARE network.file

```
clear all;close all;clc;clf;cla

flux_control_nationwide = 0 ;    %Input value between 0 and 1
flux_control_regional =[0 0 0 0 0 0 0 0 0 0 0 0]';   %Input value
    between 0 and 1
lockdown_control = 0;   %Input value between 0 and 1
Separate_north_south= 0;    %Input value between 0 and 1
target_control= 0;   %Input value between 0 and 1
vaccinationrate= 0 ;  %Amount of vaccinations per day

%% Model parameters
Provinces = {'Groningen','Friesland','Drenthe','Overijssel','
   Flevoland','Gelderland','Utrecht','Noord-Holland','Zuid-Holland
   ','Zeeland','Noord-Brabant','Limburg'};
N = xlsread('DATASHEET_SIDARE','B2:M2')'*1000 ;% Total population
    N = S + I + R
beta = 0.2; % Infection rate
gamma1= (1/14); % rate of recovery undetected: 14 days
gamma2= (1/14); % rate of recovery detected: 14 days
gamma3= (1/12.1); % rate of recovery threatend: 12.4 days
epsilon1=0.0053;% rate from infected undetected to acutely
   symtomatic: 0.3
epsilon2=0.0053;% rate from infected detected to symtomatic: 0.3
vu=0.05; % rate from infected undetected to infected detected
mu=0.0085; %*gammaa; % mortality rate 0.022*gammaa
u1=flux_control_nationwide; %nationwide control on Phi matrix
u2=flux_control_regional; %local control on Phi matrix
u3=lockdown_control;
u4=Separate_north_south;
u5=target_control
Tend=600; %simulation time
M=12;   % Amount of provinces
h=0.0481/M; % Amount of hospial beds

%% calculation of the Phi matrix
load('commute') % This loads a 12x12 matrix showing the ammou1t
   of people that move from i to j
Commute(boolean(eye(12)))=0; % the diagonals (people that work in
    their own region) are set to zero
Travel1=Commute*1000*0.9*(5/7)*(1-u1); % The travel matrix is the
    commuting data times the workday per week and the ratio of
   working from home
Travel2=bsxfun(@times,Travel1,(1-u2)');
Travel3=bsxfun(@times,Travel2,(1-u2));

if u4==1
```

```
38      Travel3=Travel3.*[ones(6,6) (zeros(6,6)+0.001);(zeros(6,6)
           +0.001) ones(6,6)]
39  end
40
41  for i=1:12
42  Phi1=eye(12).*(N-sum(Travel3(i,:)-Travel3(i,i)))+Travel3; %The
       diagonals are the total inhibitants minus the people that work
       in another region
43  end
44  for i=1:12
45  Phi(i,:)= Phi1(i,:)/sum(Phi1(i,:));  %The matrix is normalize by
       dividin each entry by the sum of the row
46  end
47
48
49  %% initialization
50
51  I0 = [0 0 0 0 0 0 0 0 0 0 1 0]'; % initial number of infected
52  S = zeros(M,1);
53  I = zeros(M,1);
54  I(:,1) = I0;
55  D = zeros(M,1);
56  A = zeros(M,1);
57  R = zeros(M,1);
58  E = zeros(M,1);
59  S(:,1) = N-I0-D-A-R-E;
60  vaccinations(:,1)=zeros(M,1)
61  kappa=0;
62
63  %% dynamics
64
65  for t = 1:Tend-1
66      N_p = Phi(:, :)' * (S(:, t) + I(:, t) + R(:, t)); %people
           that are able to move
67
68
69
70          for i=1:M
71              s2=0;
72
73
74          if sum(S(:,t))>2000000 && vaccinationrate > 1;
75              kappa=N/sum(N).*vaccinationrate;
76          else
77              kappa=zeros(M,1);
78           end
79
80                  if A(i,t)<=h
81                      mubar=mu*A(i,t);
```

```
82                  else
83                      mubar=(mu*h)+(5*mu*(A(i,t)-h));
84                  end
85
86                      for j=1:M
87                      s2= s2+beta*Phi(i,j)*S(i,t)*sum(Phi(:,j)'*I
                           (:,t)/N_p(j)); %Network infection rate (
                           Traffic taken into accou1t)
88                      end
89          %Network dynamics
90          S(i,t+1) = S(i,t)-((1-u3)*s2)-kappa(i);
91          I(i,t+1) = I(i,t)+((1-u3)*s2)- gamma1*I(i,t)-epsilon1*I(i
               ,t)-vu*I(i,t);
92          D(i,t+1) = D(i,t)+(vu*I(i,t)- gamma2*D(i,t) - epsilon2*D(
               i,t));
93          A(i,t+1) = A(i,t)+(epsilon1*I(i,t)+epsilon2*D(i,t)-gamma3
               *A(i,t)-mubar);
94          R(i,t+1) = R(i,t)+(gamma1*I(i,t)+gamma2*D(i,t)+gamma3*A(i
               ,t))+kappa(i);
95          E(i,t+1) = E(i,t)+mubar;
96          TotalI(i,t) = I(i,t)+D(i,t)+A(i,t);
97          Newinfected(i,t+1)=I(i,t+1)-I(i,t);
98          vaccinations(i,t+1)=vaccinations(i,t)+kappa(i);
99          end
100
101     end
102
103
104 %% show graphs
105
106  for i=1:M
107  fig1 = figure(1);
108   x=0:Tend-1;
109  subplot(3,4,i)
110  hold on; grid on;
111  plot(x,I(i,:)./N(i),'r',x,D(i,:)./N(i),'m',x,A(i,:)./N(i),'c',x,
        E(i,:)./N(i),'k','LineWidth',2.5); grid on;
112  xlabel('Days'); ylabel('Fraction of the population');title(
        Provinces{i})
113  end
114
115  figure(1)
116  subplot(3,4,4)
117 legend('S','I','D','E','R','E');
118
119 S_national = sum(S, 1);
120 I_national = sum(I, 1);
121 D_national = sum(D, 1);
122 A_national = sum(A, 1);
```

```
123 R_national = sum(R, 1);
124 E_national = sum(E, 1);
125 N_national = sum(N);
126 vaccinations_national = sum(vaccinations,1);
127
128  fig2 = figure(2);
129  grid on;
130  plot(x, S_national/N_national,'g',x, I_national/N_national,'r',
        ...
131       x, D_national/N_national,'m',x, A_national/N_national,'c',...
132       x, R_national/N_national,'b',x, E_national/N_national,'k','
             linewidth', 2.5);
133  xlabel('Days'); ylabel('Fraction of the population');title('The
        Netherlands')
134
135  legend('S','I','D','A','R','E')
136
137 %%
138 totalcases=round((I_national(end)+D_national(end)+...
139     A_national(end)+R_national(end)+E_national(end))-
           vaccinations_national(end));
140 totaldead=round((E_national(end)));
141 [Peakmagnitude,Peaktime] = max(I_national);
142 Peakmagnitude=Peakmagnitude/sum(N);
143 fprintf('total cases = %d,\ntotal deaths = %d,\nTime of peak = %
       dd,\nPeak magnitude = %d'...
144      ,totalcases,totaldead,Peaktime,Peakmagnitude)
145
146 %% print
147
148 % saveas(fig1,'Regional_no_interventionpol.png')
149 % saveas(fig2,'National_no_interventionpol.png')
```